NTIA Technical Report TR-11-476

Radio Channel Impulse Response Measurement and Analysis

Peter Papazian
John Lemmon

report series

U.S. DEPARTMENT OF COMMERCE • National Telecommunications and Information Administration

NTIA Technical Report TR-11-476

Radio Channel Impulse Response Measurement and Analysis

Peter Papazian
John Lemmon

U.S. DEPARTMENT OF COMMERCE

May 2011

DISCLAIMER

Certain commercial equipment, instruments, or materials are identified in this report to adequately describe the experimental procedure. In no case does such identification imply recommendation or endorsement by the National Telecommunications and Information Administration, nor does it imply that the material or equipment identified is necessarily the best available for the purpose.

CONTENTS

FIGURES

Page

TABLES

Page

RADIO CHANNEL IMPULSE RESPONSE MEASUREMENT AND ANALYSIS

Peter Papazian, John Lemmon[1]

This paper describes radio channel sounding measurements and analysis using pseudo-noise (PN) codes. It presents a channel sounding model and shows how channel measurements can be made. A measurement system is described that can be implemented using a combination of radio frequency (RF) hardware, high speed analog to digital converters (ADC), and signal processing software. Sampling requirements and models for describing the stochastic nature of the radio channel are discussed. Typical signal outputs of a PN channel sounder from the laboratory and from field measurements are shown. The field measurements are used to show how channel sounding data can be processed to develop a power law model of short-range communications. This model can be used for a statistical estimation of received power and interference analysis.

Key words: channel model, channel sounding, impulse response, multipath, propagation, RF

1 INTRODUCTION

Propagation measurements are used to analyze the performance of radio systems and to develop models for interference and link budget analysis. To predict the performance of mobile communication systems it is necessary to measure fast fading caused by multiple received signals traveling over different paths, or multipath. The fading caused by multipath is sometimes called multiplicative effects since the signal power in the frequency domain can be multiplied by a frequency selective or flat fading scaler or complex factor. This is different from noise, which is additive in nature. To characterize multipath and fast fading waveforms, the radio channel impulse response is measured. Because signal fading and multipath are important for both interference studies and receiver and system performance studies, radio channel impulse response measurements and systems are commonly employed for radio propagation measurements. Impulse response measurement is important when communication systems are digital because the impulse response can be used to determine inter-symbol interference which can cause decoding errors.

In principle, the most straightforward way to measure the the impulse response of the channel would be to transmit an impulse-like signal over the channel and measure it at the receiver. This approach has actually been used [1], but requires large peak powers and radar-like equipment. An alternative approach is to use a pseudo-noise channel probe, whereby a band-limited noise signal is transmitted over the channel. The main idea is that although noise is not impulsive, its autocorrelation function is, so that the impulse response can be measured by correlating the received signal with a copy of the transmitted noise.

[1]The authors are with the Institute for Telecommunication Sciences, National Telecommunications and Information Administration, U.S. Department of Commerce, Boulder, Colorado 80305.

This approach was first used by Cox [2] and then used at the Institute for Telecommunication Sciences (ITS) by Hubbard [3],[4],[5]. These probes performed the correlation using analog processing. A copy of the code was made to slowly drift by the received signal and the integration was performed by a low-pass filter. Fifteen years ago, ITS also developed [6] and patented [7] a digital probe, which samples at IF and performs the correlation in software. The advantage of the digital probe is its linearity and its ability to sample the channel more quickly than a sliding correlator. This allows a statistical analysis of mobile measurements in the VHF, UHF, and SHF bands. The original digital probe has more recently been modified to: record continuously for communication systems modeling, record multiple channels for MIMO applications, and record at multiple frequencies and channel bandwidths simultaneously.

The purpose of this report is to present an up to date account of the ITS channel probe, its associated signal processing, and the sampling methods needed to measure the mobile radio channel. It is organized as follows. Section 2 presents the radio channel model and shows how a pseudo-noise signal is used to determine the channel impulse response. Section 3 discusses pseudo-noise (PN) codes, their properties and measured examples of their characteristics. Section 4 shows a generalized RF architecture for a digital channel sounder. Section 5 discusses the sampling requirements needed to accurately measure mobile channel characteristics. This section also introduces models used to describe mobile channels. Section 6 outlines the signal processing methods used by the channel sounder. Section 7 summarizes statistical distributions commonly used to describe radio propagation measurements. The section then shows how processed data is used to characterize fast fading, and how the fast fading data is used to estimate mean signal strength over a small area. This result leads to the calculation of the slow fading distribution needed for a power law channel model. Conclusions regarding the PN channel sounding method and the power law model are given in Section 8.

2 PSEUDO NOISE CODE SOUNDING

2.1 Radio Channel Model

The impulse response is a transfer function which relates the received signal to the transmitted signal. This process is modeled as a linear system, so the channel model can be written as

$$y(t) = x(t) * h(t) + n(t), \tag{1}$$

where $x(t)$ is the transmitted signal, $y(t)$ is the received signal, $h(t)$ is the impulse response, $n(t)$ is additive noise and $*$ is the convolution operator.

Correlating each side of (1) with $x(t)$ leads to

$$R_{xy}(\tau) = h(\tau) * R_{xx}(\tau), \tag{2}$$

where $R_{xx}(\tau)$ is the autocorrelation function of $x(t)$, R_{xy} is the cross-correlation function of $x(t)$ and $y(t)$, τ is the delay time, and $n(t)$ and $x(t)$ are assumed to be uncorrelated.

2.2 Considerations for Correlation Processing

If the channel impulse response changes slowly with respect to the time interval required to measure the correlation function, then both (1) and (2) can be used to measure $h(t)$. In addition, if the correlation function R_{xx} of $x(t)$ approaches a delta function then R_{xy} is a good approximation of $h(t)$. This condition can be realized using pseudo-noise (PN) codes.

2.3 Pseudo-Noise Code Channel Sounder

Equation (2) is realized by transmitting a PN code through a channel and correlating the received signal with the transmitted PN sequence. To make channel measurements at radio frequencies, the PN code is used to modulate an RF carrier. After transmission through the radio channel, this signal is then down-converted to baseband where the correlation process can be used to calculate R_{xy}. These data are then stored as complex impulse responses (CIR) for further processing.

The ability to vary bandwidth (BW) and maximum delay are important characteristics of PN sequence sounders. The sounder also has a processing gain which can be increased by using longer code words. The processing gain reduces transmitter power requirements. As the sounder's bit rate is increased its time resolution also increases and this requires larger transmission $BW's$ and digitization speeds. These features can be used to limit the high power and bandwidths which would be required if unit impulses were transmitted instead of PN sequences.

3 PSEUDO NOISE CODE PROPERTIES AND GENERATION

3.1 Code Properties

At this point, it is important to know more concerning PN sequences and their correlation properties. The most useful feature of these codes for channel sounding is that their autocorrelation functions approximate a bandlimited version of $i(t)$, the unit impulse function.

The PN codes used in the the channel sounder are maximal length sequences. The generalized properties of maximal length sequences can be found in Dixon [8] and Peterson [9]. The following list summarizes these properties:

1. The code repeats every $2^r - 1$ bits and can be produced using a linear feedback shift register, where r is the number of shift register stages (Figure 1).

2. The number of ones in a sequence equals the number of zeros to within one bit.

3. The PN sequences autocorrelation function is a triangular waveform. The waveform is 2 bits wide and $2^r - 1$ units high with a base value of -1 (Figure 2).

4. Autocorrelation of a maximal length code is such that all values of the phase-shifted correlation value are -1, except for the 0 time lag values which varies linearly from -1 to a peak of $2^r - 1$ (Figure 3).

5. The correlation processing gain in dB is $20log_{10}(2^r - 1)$. The ratio of the correlation peak to the average value of the correlation tail should be equal to the theoretical value. If the peak of the correlation tail is measured instead of its average value, this ratio can be used to determine the performance of the code generator. This ratio is referred to as the interval of discrimination (IOD).

6. The correlation power signal-to-noise when the received signal equals the receiver noise power is $10log_{10}\ (2^r - 1)$. This is called the processing gain.

7. A modulo-2 addition of a maximal length code with a delayed replica of itself results in a delayed replica of the original code. This can be used to produce delayed autocorrelation sequences.

3.2 Adjusting Code Properties for Channel Sounding

For channel sounding applications, important characteristics of the impulse response can be adjusted to match the propagation channel of interest by changing the bit rate of the code (BR) and the register length (r) of the code generator. Important channel sounder properties are its time resolution (t_{min}), maximum delay (t_{max}), bit period (Δt_b), null-to-null bandwidth (BW), number of bits per code word (N_{Bit}), correlation peak to average noise (C/N), the processing gain which is the ratio of the correlation peak to tail when the received signal equals the receiver noise ($S/N = 1$), and the interval of discrimination IOD.

These properties are all adjusted by changing the two fundamental properties of the PN code generator, the register length r and bit period $\Delta t_b = 1/BR$) using the following relationships:

1. $N_{Bits} = 2^r - 1$.
2. $BW = 2/\Delta t_b$.
3. $t_{min} \approxeq 2\Delta t_b$.
4. $R_{xy}\, correlation\, gain = 20log_{10}(N_{Bits})$.
5. $R_{xy}\, processing\, gain = 10log_{10}(N_{Bits}), when\, S = N$.

3.3 Pseudo Noise Code Generation

PN sequences can be generated using a linear shift register with feedback. Figure 1 shows a 9-stage shift register with feedback taps 4 and 9.[2] The design and modulo-2 addition can also be used to generate a software copy of any pseudo-noise code if the register length and feedback taps are known. These parameters for different length codes can be found in Dixon [8] and Peterson [9]. A computer-generated code can then be used to perform software-based correlation of the received waveform at baseband as described in Section 6. In practice, the hardware code generator has been replaced by memory usually in an FPGA or digital IO generator. The code can be loaded into memory and then played back repetitively at the desired bit rate. The memory based code generators have less distortion, which is usually seen as ringing in the bit sequence waveform. The ringing can cause spurious correlation peaks. It has been found that the impulse response of a memory based code generator has a larger IOD then ones produced using a register based code generator.

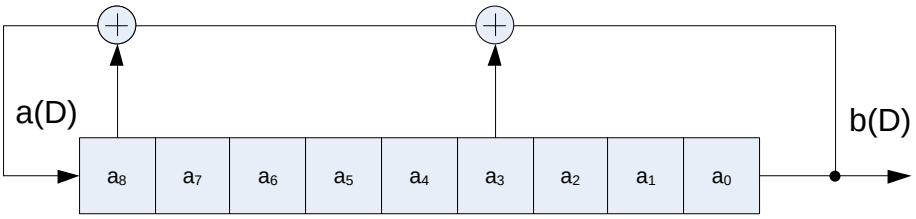

Figure 1. A 9-stage linear shift register with feedback at taps 4 and 9. The initial load is polynomial $a(D)$ and the output is the polynomial $b(D)$. The initial load polynomial can be any sequence of ones and zeros except for the sequence containing all zeros. For a more detailed description of these polynomials see Dixon [8] and Peterson [9].

Figure 2 is a sketch that illustrates the cyclic autocorrelation squared of a PN code generated by a shift register of length r and clock period τ_0. The correlation peak has a value of $(2^r - 1)^2$ and is cyclic with period $(2^r - 1)$. The correlation peak is a triangular waveform whose base is two

[2]This shift register configuration is commonly used in the ITS channel probe for mobile channel sounding.

bits or clock periods wide. The peak interval of discrimination (IOD_{pk}) for the correlation is the distance between the correlation peak and the peak value of the noise in the correlation tail.

Figure 3 shows the first 50 points of a computer-generated autocorrelation for a 511 bit (r=9) maximal length sequence. This is an ideal computer-generated output with no noise and the autocorrelation is not squared. The peak is 511 bits high and the tail is -1 (PN property 4). Figure 4 shows the magnitude squared of this ideal autocorrelation on a dB scale. We see the correlation peak is 54 dB above the tail (PN property 5). Later in the report we show measured PN correlations with noise for comparison.

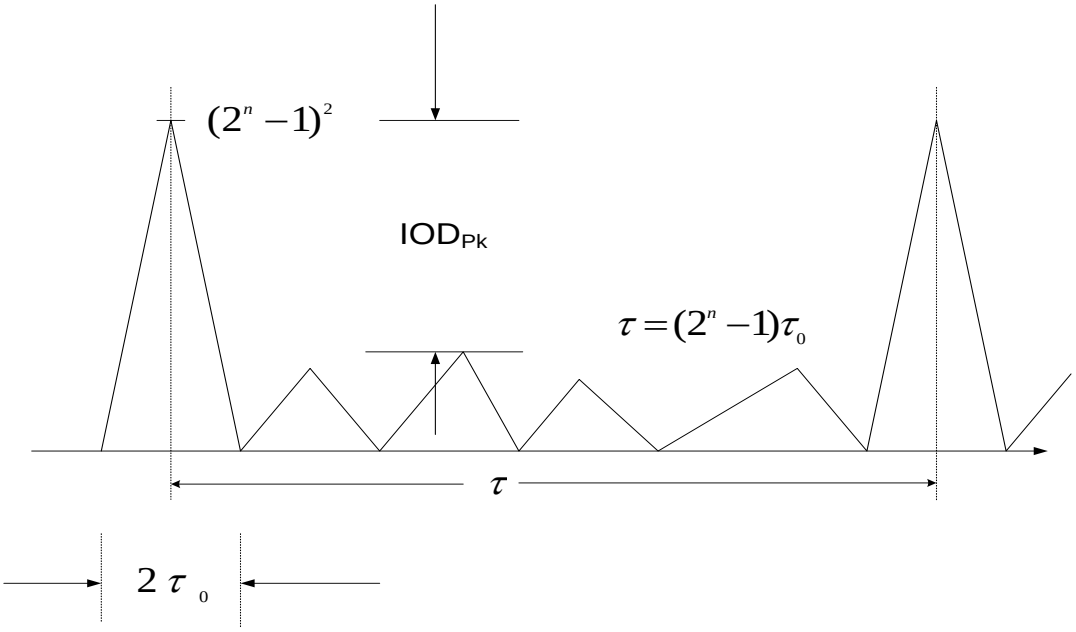

Figure 2. An impulse response drawing. The drawing shows the cyclic autocorrelation of an maximal length sequence squared of degree n in the presence of noise. In this graphic $\tau_0 = \Delta t_b$, the bit period. The autocorrelation has a triangular waveform whose base is $2\tau_o$ or 2 bits wide when displayed on a linear scale.

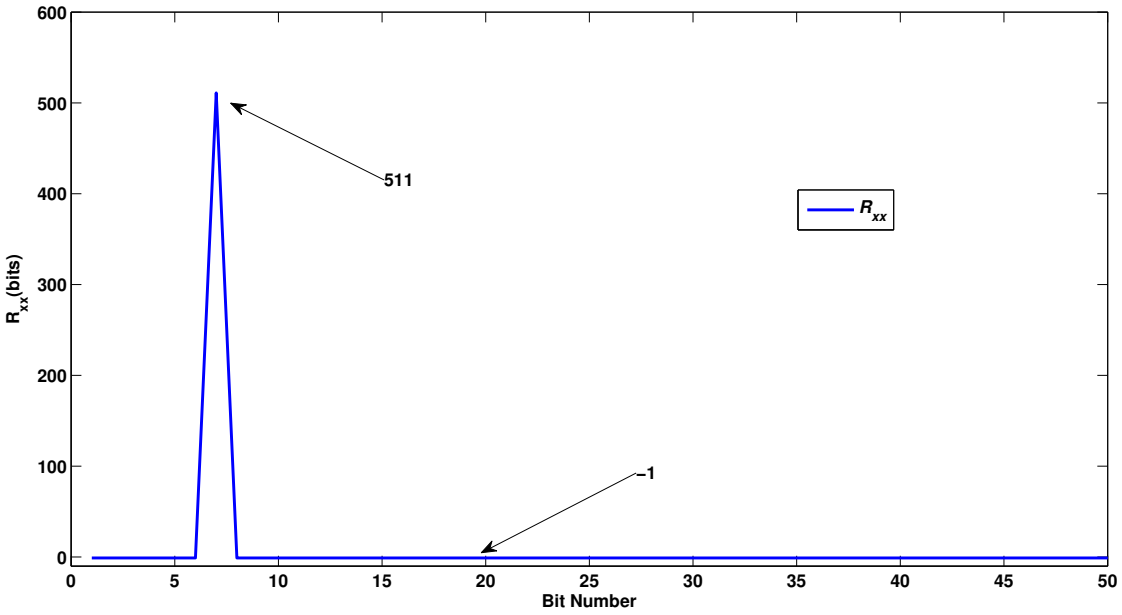

Figure 3. The computed autocorrelation for the maximal length sequence with $r = 9$, and feedback taps at registers 4 and 9. The peak value is equal to the number of bits in the sequence and the minimum value is -1.

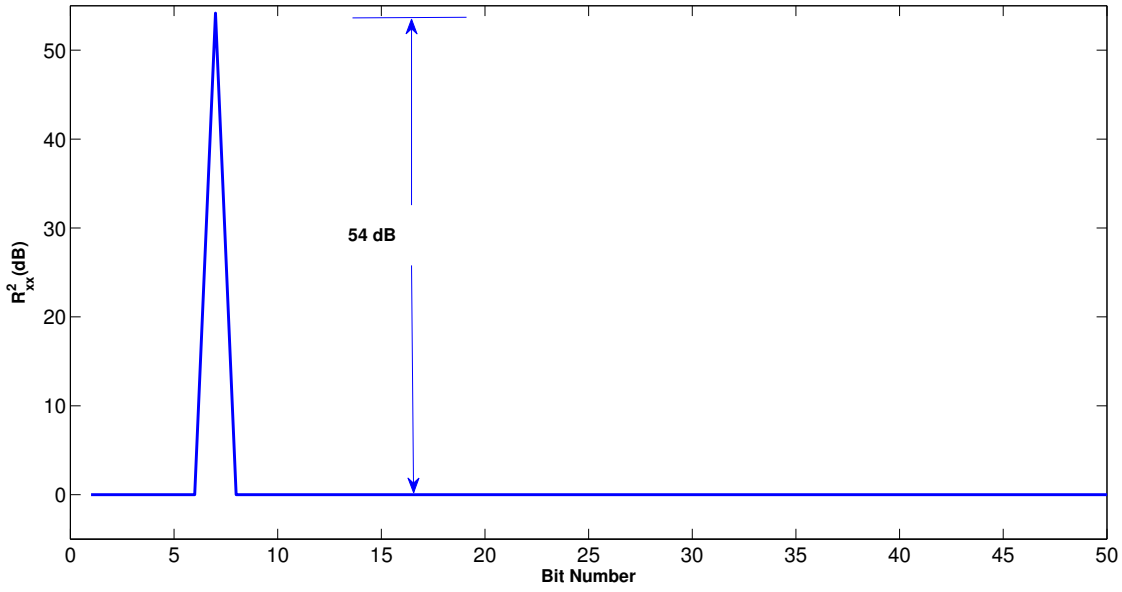

Figure 4. The computed autocorrelation power on a log scale for 511 bit maximal length sequence. The ideal response is 2 bits wide with a peak-to-tail ratio of 54 dB.

4 CHANNEL PROBE ARCHITECTURE

4.1 Overview

A channel probe can be constructed using a heterodyne radio transmitter and receiver. Figures 5 and 6 show block diagrams of such a system. The transmitter (Figure 5) consists of a pseudo-noise generator and analog conditioning circuit to change the PN code into a $\pm 1V$ waveform. This waveform can then be filtered at baseband to limit the transmission bandwidth to the first null in its power spectrum. This null occurs at the bit rate frequency. The filtered waveform is then used as input for the IF port of a mixer. The mixer is used to bi-phase shift key (BPSK) modulate the RF carrier signal. The final stages of the transmitter include the power amplifier and an additional low-pass filter (LPF) used to remove harmonics from the transmitted signal.

The receiver (Figure 6) consists of a front-end bandpass filter used as a pre-selection filter followed by a low-noise amplifier (LNA), a down-conversion section and band-pass filter (BPF). After amplification a second mixer is used to down-convert to the intermediate frequency (IF). The local oscillator frequency is set so the IF is equal to the bit rate of the pseudo-noise code. This allows synchronous sampling at an integer multiple of the code rate. Here synchronous means phase synchronous with the bit period. This implies each bit will be digitized with the same number of samples per bit. The Nyquist rate is set by bandlimiting the spectrum of the IF signal at its first null. These choices also allow variable code rate reception with over-sampling if the additional code's bit rates are integer divisors of the code with the largest BWs or bit rate. A low-pass filter is used to prevent aliasing and the band-limited IF signal is then passed to a analog-to-digital converter (ADC) for sampling and storage.

As in all data sampling procedures, care must be taken when selecting the appropriate sampling rates. This is necessary not only to prevent aliasing but also to obtain a sufficient number of samples when the radio channel is stationary so one can estimate channel parameters accurately. Channel sampling requirements will be discussed in Section 5. For now, we will deal with the measurement of a single channel response and the hardware which can be used to make this measurement. It should be noted that the antennas are part of the radio channel. If a particular channel or type of system is to be measured, the antennas should be chosen appropriately to match the desired system and radio channel.

4.2 Radio Frequency Hardware

The block diagrams of the multi-channel probe used to make measurements presented in this paper are shown in Figures 5 and 6. In this case hardware was chosen for simultaneous measurements in multiple frequency bands. Because the radio bands of interest had variable BWs available, the probe was configured for multiple bit rate and carrier frequency operation. The multi-channel PN probe can also be configured to record multiple channels at the same frequency. This configuration was developed by Papazian and Gans [10] for MIMO channel measurements. It required a code generator capable of transmitting multiple orthogonal codes, one for each transmitter antenna element. This configuration enabled measurement of the MIMO channel response matrix.

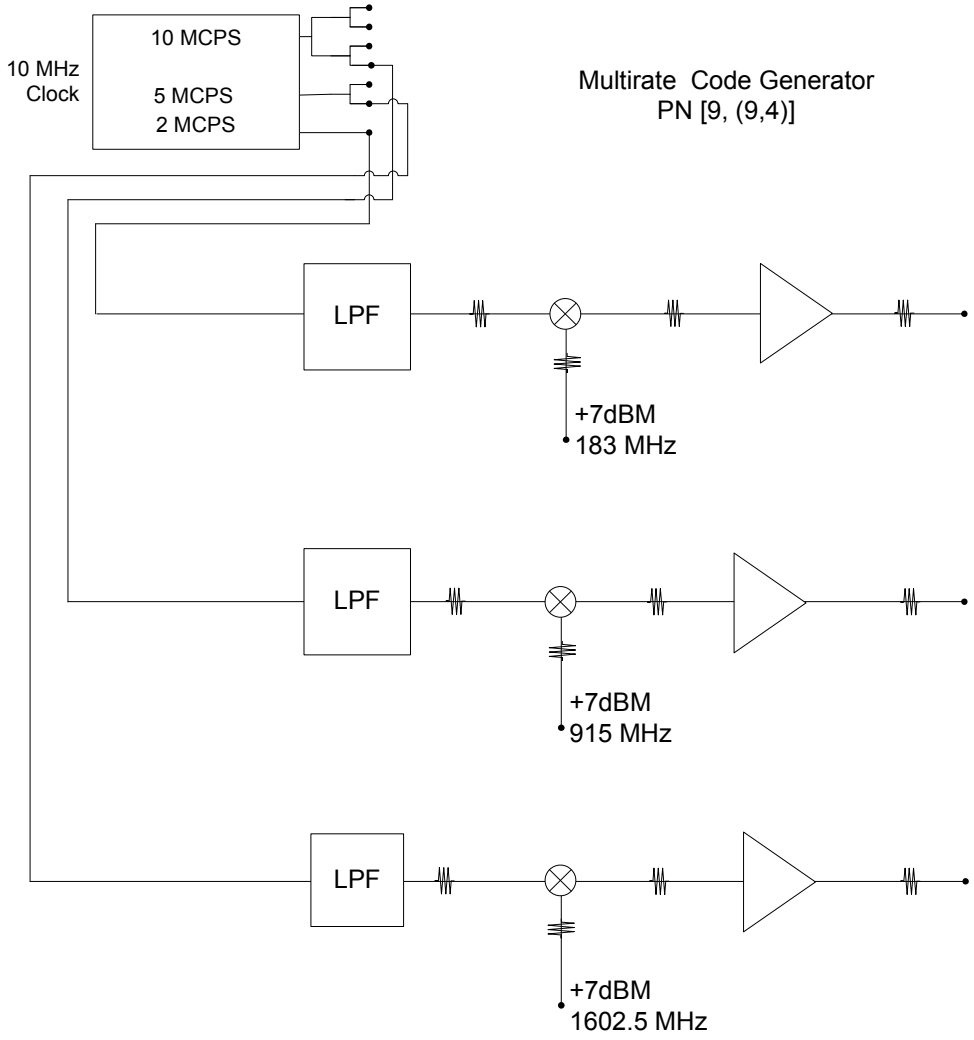

Figure 5. A 3-channel transmitter with variable PN code rates.

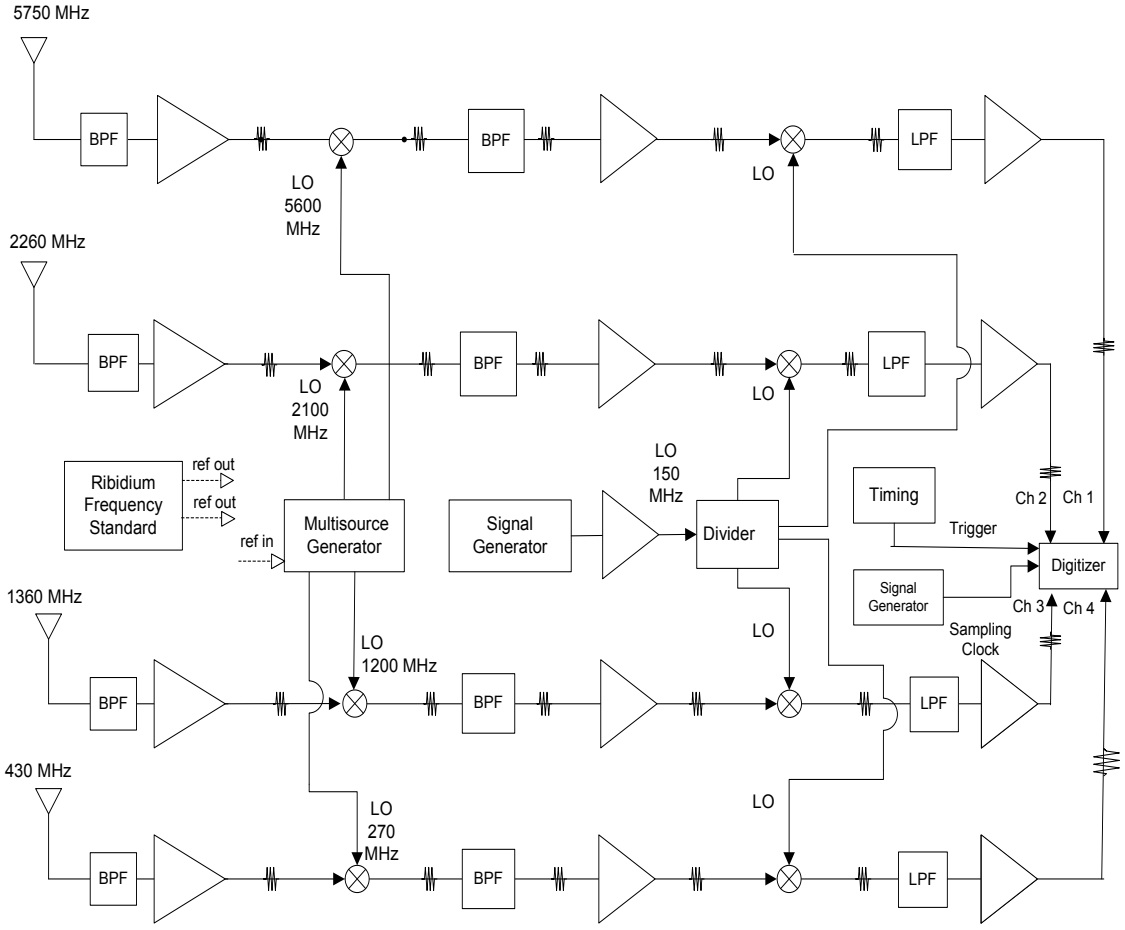

Figure 6. A multichannel dual down-converting receiver used for multi-rate channel sounding.

4.2.1 Calibration Measurement Example

Figure 7 is a calibration measurement for one of the probe channels. This data is used to check the probe operation as well as to measure the probe power calibration constant. The figure shows a power delay profile (PDP), calculated as $|h|^2$, using a digitized IF signal at a high S/N. Several important parameters of the PDP are measured from this graph. These include the peak interval of discrimination (IOD_{Pk}) and the average interval of discrimination (IOD_{Avg}).

In this test, a 511 bit code was transmitted at 10 MB/s and the codeword was synchronously digitized at 40 MHz yielding 4 samples per bit. This rate is the Nyquist sampling rate for the bandpass IF signal ($BW_{if} = 20$ MHz). Referring to the PN properties of section 3, we can calculate the ideal result for the IOD_{Avg}, which is the ratio of the PDP peak to the average value of the PDP tail. The ideal IOD_{Avg} is 54 dB. The measured value of 53 dB is close to the ideal and is a good indication that the correlation processing is working as expected. An important figure of merit for the probe implementation is also IOD_{Pk}. Correlation noise spikes, which limit IOD_{Pk} can be caused by distortion in the PN sequence created in the PN generator, non linearities in the RF system such as intermodulation distortion, mixer port to port coupling, and RF leakage between channels. The measured value of 47 dB is very good and ensures that noise spikes will not be mistaken for multipath when delay spread is calculated.

The probe's input RF power level is adjusted using precision attenuators and measured with power meter. When the RF power level is decreased by 10 dB, the the received power calculated using the PDP will also decrease by 10 dB if the probe is operating in its linear range. When the S/N (N = receiver noise power) is high the PDP peak is reduced by 10 dB when RF signal is reduced by 10 dB. The average level of the PDP tail also drops by 10 dB indicating the tail is above the receiver noise floor and IOD_{Pk} remains constant.

As the RF power into the receiver is further attenuated the tail of the PDP will drop to the level of the receiver noise floor. At this input power level or less, the PDP tail level remains constant while correlation peak will decrease in amplitude relative to the PDP tail.

When the RF input power equals the receiver noise power, we expect the correlation peak to be 27 dB above the noise (Property 6). This is called the correlation processing gain. Figure 8 shows such a case for IOD_{Pk} measured during the calibration process.

Figure 9 is a measurement example from an urban area of downtown Denver (blue curve) with a calibration record (red curve) superimposed. The measured PDP from Denver shows multiple reflected signals of decaying amplitude. The PDP has an approximately exponentially decaying tail which is typical of urban areas. The red curve gives a good idea of the probe resolution relative to a typical urban multipath record. The timing circuit used to trigger the digitizer is set so that the calibration PDP peak (red curve) is delayed by 2.2 μs. This is done so that the start of the PDP can be seen clearly. The relative time of arrival between the first peak of the downtown PDP and the calibration PDP is the time of flight. It can be used to calculate the radio path length of the downtown measurement. The radial distance between the transmitter and measurement location is determined using the GPS coordinates.

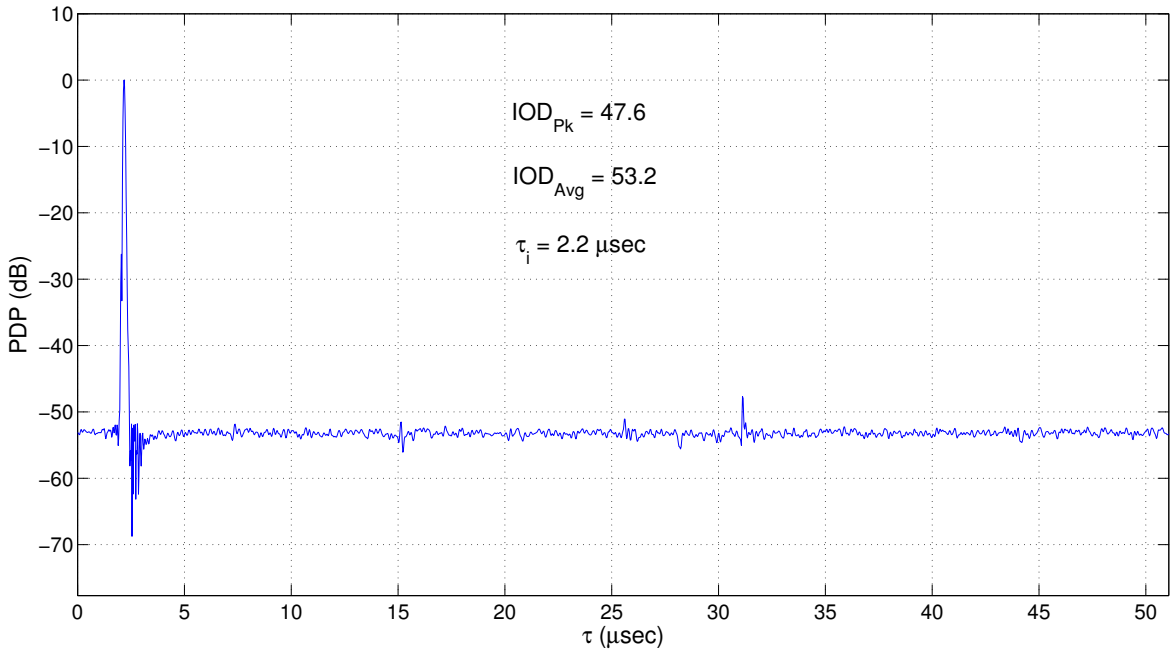

Figure 7. The PDP of the transmitted maximal length sequence. Note that the units of the abscissa have changed from bits to μs. The code was transmitted at 10 Mb/s and the length of the 511 bit codeword is 51.1 μs. The channel is coaxial cable and this is a calibration measurement. The codeword is delayed 2.2 μs relative to the digitizer trigger.

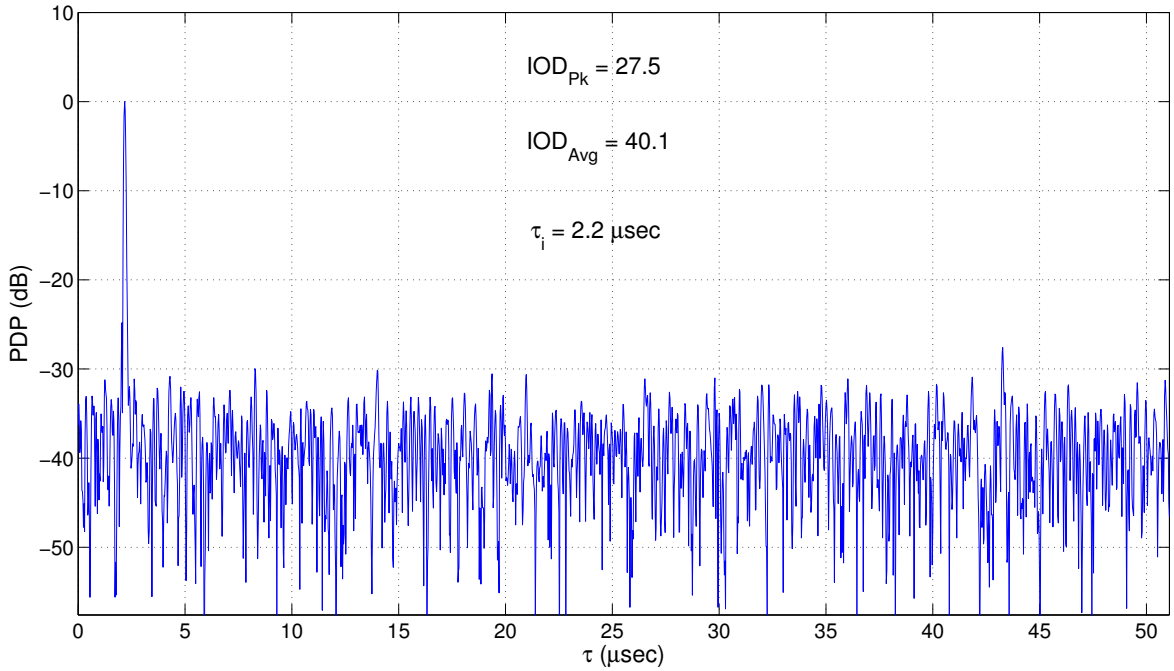

Figure 8. The PDP when the input signal power equals the noise power. The IOD_{Pk} is 27 dB.

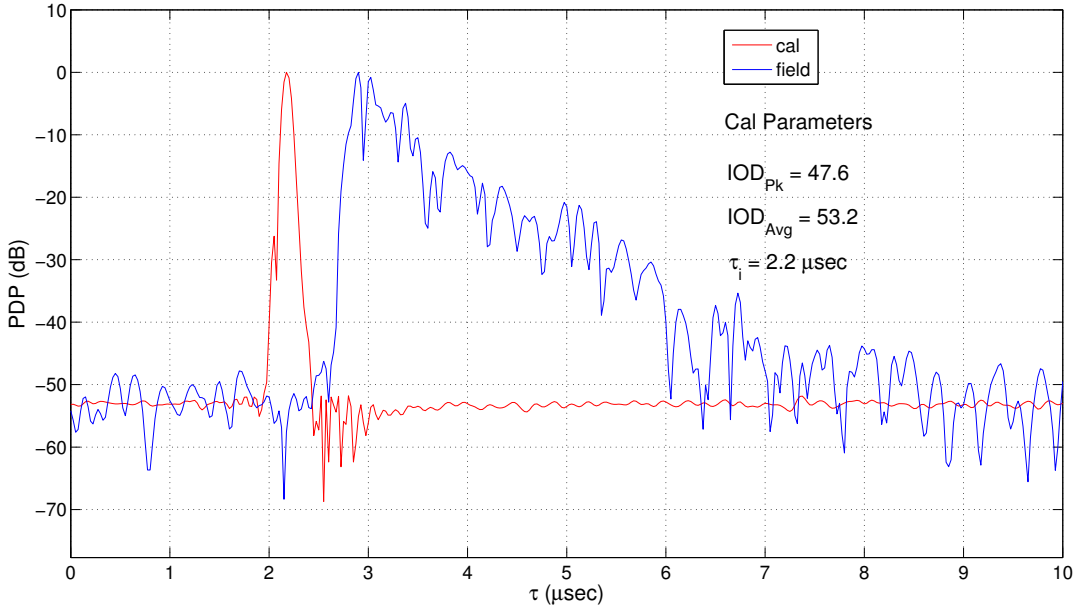

Figure 9. A PDP measured in the downtown area of Denver, CO shown in blue. This radio channel impulse is typical for built up areas with multipath signals. The channel sounder calibration response is shown in red. The red curve illustrates the channel sounder resolution and zero delay time. The the calibration signal IOD_{Pk} is 47.6 dB and its delay is $\tau_i = 2.2\mu$s. The relative delay between the two PDPs can be used to measure the radio path lengths.

5 MOBILE RADIO CHANNEL SAMPLING

5.1 Background

Propagation measurements are used to characterize the radio channel and quantify how channel impairments affect radio performance. The channel impulse response is measured because it provides a complete description of the radio channel and a complete characterization of propagation impairments. The channel impulse response $h(t,\tau)$ is a function of t and τ, where t is the time at which the measurement is performed and τ is the delay of the channel response. For the mobile channel $h(t,\tau)$ is a stochastic function of t for each value of τ. Therefore, at each measurement delay τ, subsequent impulse measurements form a random sequence. The time between impulse measurements determines the measurement interval when characterizing this random sequence. This time between impulses in the channel sounder is t_{bi}; the frequency of this time interval is also referred to as the the channel sampling rate. The maximum value of t_{bi} for channel sounding data is determined using the Doppler BW of the channel and the Nyquist sampling criteria.

In this report, the method used to determine t_{bi} will be referred to as the Doppler sampling rule. The objective of this section is to explain how this rule satisfies statistical sampling requirements of the mobile radio channel.

It should be noted that the sampling rule is necessary when measuring the average received power over small areas in addition to being required for measuring $h(t,\tau)$.[3] The average power value over small areas is called the slow fading signal and the sampling rule applies to narrowband as well as wide band measurements.

There are two important physical characteristics of the mobile channel which should be quantified before sampling requirements can be determined. The first characteristic is that the mobile channel is non-stationary. The second is that the channel may be experiencing random fading and consequently rapid and random power level changes (fast fading). The first condition, non-stationarity, requires the collection of a minimum number of uncorrelated samples *when the channel is stationary*. This is necessary so that the mean value of the received power can be estimated accurately. The second physical property, rapid power changes, requires sampling quickly so that fast fading can be measured. It will be seen by reviewing the literature, and by an example at the end of this section, that the Doppler sampling rule can be used to determine the channel sampling rate and that the configuration of the channel probe satisfies the fast sampling requirement.

5.2 Sampling Requirements Overview

Mobile channel characteristics and sampling methods have been studied and reported by Jakes, Parsons, Lee and Steele [12]–[17]. The following is a summary of their findings.

[3]The delay-spread function $h(t,\tau)$ is one of the Bello [11] system functions used by Cox [2] to determine the channel scattering functions. Using these functions and their Fourier transform duals, a description of the dispersive nature the channel in the time-delay, delay-Doppler, frequency-Doppler and frequency-time domains can be displayed. These functions can then be used to calculate any statistical metric needed to characterize a band limited mobile radio link. The functions are used to specify tapped delay line filters for equalizers and the weights of these filters commonly provide descriptions of the radio channel for standards work.

The number of uncorrelated samples needed for estimating mean power has been analyzed by both Parsons and Lee. They came up with slightly difference answers. Parsons determined that 57 samples are needed to estimate mean received power with 1 dB of accuracy, when using a linear receiver, in a Rayleigh channel. Lee determined 40 samples were necessary for an accuracy of 1 dB in the estimate of the mean power in a Rayleigh channel.

The stationarity interval for the channel is variable and it depends upon the geometry of nearby scatterers. It has been reported by Steele, Parsons and Lee [15]–[17] to be a few tens of carrier wavelengths for cellular radio studies. Steele also reported that the RMS averaging window in micro-cells for fast fading is between 4 λ_c and 10 λ_c.

For cellular radio applications, the correlation distance between samples in a Rayleigh channel is about 0.5 λ. This distance has been determined through calculations and measurements by Parsons and Lee.

The following subsection provides additional background about the statistics of the mobile radio channel necessary for measuring and analyzing power data.

5.3 Fast Fading, Slow Fading and Mean Power

The received power signal can be separated into two stochastic components which describe the radio channel: the fast fading signal and the slow fading signal. Fast and slow fading are referred to separately because they are caused by independent processes and are described using different statistical distributions.

The fast fading signal and the fading rate are related to the mobile velocity and the carrier wavelength. Fast fading is caused by multipath interference when delayed signals of different amplitudes and phases add either constructively or destructively. This causes interference patterns which the mobile unit drives through, leading to a fast time variability of the received power level. The spatial variability of this component is on the order of the carrier wavelength.

The slow fading component is primarily a consequence of shadowing by buildings, terrain, and vegetation. The shadowing lasts for longer distances or periods of time. This component can be determined by averaging the fast fading data over small intervals when the channel is stationary. During these intervals the received power will have a constant mean value.

To measure the received signal power accurately, it is necessary to sample the channel at the proper rates. A fast power measurement is required so that the fast fading signal can be determined. Also required are the correct channel sample rate (time between power measurements) and an averaging interval so the slow fading signal can be determined.

5.4 Sampling Considerations and Requirements

The general problem is to represent a continuous time function as a time series of digitized values. The standard method is to determine the maximum bandwidth (BW) of the continuous signal and

then set the minimum sample rate at the Nyquist rate for this BW. Since this BW is determined by the fast fading component of the received signal, we should determine the maximum BW of the fast fading signal. Measurements and models of fast fading have been given by Jakes [12], Parsons [13] and others.

We know from Jakes that the BW of the RF signal is equal to the difference between the maximum and minimum Doppler frequencies. The RF BW and necessary sample rate can be determined using the Doppler equation,

$$f_d = \pm \mathrm{v}/\lambda_c. \tag{3}$$

In this equation, v is the closing velocity between the mobile and reflectors and λ_c equals the carrier wavelength. The Doppler bandwidth (BW_d) is $2\mathrm{v}/\lambda_c$. The Nyquist sample rate is $4\mathrm{v}/\lambda_c$. This is the minimum channel sample rate that should be maintained for both wideband and narrowband measurements.

After fast fading has been measured, the slow fading signal is calculated by averaging the fast fading signal while the channel is stationary. The number of uncorrelated samples needed for accurate estimate of the mean in Rayleigh fading channels has been studied by Parsons [13] and Lee [14]. Again, *Parson calculates the 90% confidence interval for 1 dB accuracy and determines it requires 57 samples for a linear receiver. Lee found that about 40 samples were needed to achieve 1 dB of uncertainty in calculation of the mean power.*

The interval over which the received signal is stationary is dependent upon the scattering environment. When more scatterers or clusters of scattering objects are present, such as in urban areas, the stationarity interval for averaging data has generally been found to be a few tens of wavelengths [13],[15]–[17].

Another important consideration when measuring fast fading is the length of fades. The length of fades in wavelengths has been found to be dependent on fade depth. It can vary from .01 λ for a 30 dB fade to 0.48 λ for shallow fades [13].

This information will be used when demonstrating how the Doppler sampling rule determines the minimum channel sampling rate.

5.5 Multi-Rate Receiver Configuration

It is desirable to compare multiple radio bands simultaneously. To accomplish this, a multi-rate or multi-bandwidth sounder is necessary. This is required because different radio bands are allocated different bandwidths. To record multi-rate data, it is important to determine a common digitization sample rate for all channels as well as a common record length for the digitizer. This determination is quantified at the beginning of the sampling examples. To understand the sampling examples, the acquisition mode for the receiver is explained and pertinent parameters are summarized.

Impulse data are collected using the multi-rate receiver configured for burst mode acquisition. A burst is defined as a grouping of impulse records. An individual impulse record lasts for a short

time period, but the records in the burst are purposely separated by a longer time interval. This longer time is called the time between impulses (t_{bi}).

The time period of the data burst equals the number of impulses per burst (N_B) times t_{bi}. The channel sample rate ($1/t_{bi}$) should be the minimum sampling rate required by the Doppler rule. As we will see, this rate will enable collection of the required number of uncorrelated samples.

The digitizer clock (sample) rate ($1/t_i$) is determined by the BW of the PN spectrum. This sample rate is about 4 orders of magnitude faster than the channel sampling rate ($1/t_{bi}$). Each impulse recording is synchronized with the PN code transmission and typically lasts one period of the PN code word. It requires one codeword or impulse record to obtain a power sample. The time it takes to acquire these fast power readings depends upon the PN code rate and the code length. It will be seen that impulse records are short, and that the resulting power measurements during a burst can be considered instantaneous power readings. The time period to acquire a power reading is quantified in the next section.[4]

The number of samples per impulse (record length) is NPN. This number is determined by the number of bits in the PN code word and the number of samples per bit.[5]

Lastly, the time between bursts (groups of impulse data), is much longer (seconds) and is set using the computer clock. This less precise timing is used only to perform a random sampling of the survey area. This time period is not important for the sampling example.

5.6 Sampling Example

The following examples illustrate how the record length and channel sample rate are determined when using the multi-rate receiver.

1. The largest BW channel is 20 MHz. To measure its characteristics, a 511 bit code word is transmitted at 10 Mb/s and recorded using an IF of 10 MHz.

   To avoid interfering with adjacent bands, the transmitted signal is filtered at the null of its first lobe. For the 10 MHz bit rate nulls occur at $\pm$ 10 MHz. This determines the required IF BW of 20 MHz and a sample rate of 40 MHz to meet the Nyquist criterion. Since this is 4 samples per bit (S_B), NPN is 2044 samples.

2. The smallest BW channel is 4 MHz. A 511 bit code word is transmitted at 2 Mb/s and received using the same 10 MHz IF. It is recorded simultaneously using a multi-channel receiver and a multi-channel digitizer.

   Since the digitizer can only run at one rate, the sample rate (SR) must be 40 MHz as required by the 10 Mb/s channel. When digitizing the 2 Mb/s code, this means there are

[4]The bit rate (BR), digitizer triggers, sampling clock, and carrier frequencies are set using rubidium frequency standards. This ensures that phase stability can be maintained during the survey period.

[5]The PN parameters, bit rate (BR) and code length (N_{Bits}), are also important for determining the time resolution, maximum delay and processing gain of the data.

20 samples per bit. The code word is also 511 bits long and NPN is now 10,220. This is the record length required by the digitizer. Because this sampling rate is not required for the 2 Mb/s measurement, the signal can be decimated before the correlation processing. Its PN power spectrum is also filtered at its first null when transmitted to avoid out of band interference. This filter determines the signal BW. After filtering the IF, BW of the 2 MB/s channel is 4 MHz. The sampled time series is down-converted to baseband, low-pass filtered at 2 MHz and decimated by a factor of 5. After decimation and filtering for both channels, NPN_d is now 2044 (see Table 1).

Table 1. The multi-rate receivers samples per bit and record length, before and after decimation.

$BW(MHz)$	S_B	NPN	NPN_d
4	20	10220	2044
20	4	2044	2044

The record length can now be used to determine the time needed to make a power measurement for the 10MB/s channel.

Consider the following PN probe example: A measurement vehicle is moving at 15 m/s while making impulse response measurements. The PN bit rate is 10 MB/s and the code is generated using a 9 tap shift register resulting in a 511 bit codeword. The carrier frequency is 5.75 GHz. First we calculate the length of the PN code. This determines the time required to make a power estimate and the distance the mobile travels during this measurement. From the bit rate and register length we can calculate the following table.

Table 2. Measurement period and distance for a 10 MB/s code with a vehicle velocity of 15 m/s and $f_c = 5.75$ GHz.

N_{Bits}	$t_i(\mu s)$	$d(mm)$	$d(\lambda)$
511	51.1	0.8	0.01

We see that power measurements are made in 51.1 μs and that the mobile travels one hundredth of a carrier wavelength during this measurement. The interval for a 30 dB fade has been measured by Parsons [13] to be as small as 0.01 λ. If the mobile is in a deep fade that lasts for a small fraction of a wavelength, the short time period of a PN code word makes it is possible to measure the power level of the faded signal (Table 2).

In section 5.2 it was reported that in urban areas the channel remains stationary for a few tens of carrier wavelengths.

The averaging time (t_a), which is the time it takes to cover this distance, depends on the mobile speed as well as the carrier frequency. The following equation is used to determine a time range

for averaging mobile measurements:

$$10\lambda_c \leq vt_a \leq 40\lambda_c. \tag{4}$$

The averaging time (t_a), divided by the time between channel measurements (t_{bi}), is then used to quantify the number of power samples that can be used to determine the PDF of the fast fading signal and then averaged when calculating is mean value.

The channel sample rate ($1/t_{bi}$) should enable the collection of the maximum number of uncorrelated samples when the channel is stationary. The requirement for independent samples, combined with the limitation on sampling period imposed by the non-stationarity of the channel, limit the accuracy of mobile measurements. Sampling faster than required by the Doppler rate doesn't necessarily improve the accuracy of channel statistics, because the samples can become correlated. Sampling slower than the Doppler rate will limit measurement accuracy because not enough samples may be acquired to accurately measure the PDF or its moments. To increase the accuracy of the fast fading PDF, it is usually normalized by its mean value and summed. This also requires an accurate mean value and the use of the minimum Doppler sampling rate. *Sampling at less than the Doppler rate will limit the accuracy of the mean value estimate or slow fading power estimate as it will limit the number of uncorrelated samples collected for averaging.*

When the Nyquist rate for the Doppler BW is used to determine the maximum time between impulse recordings (power measurements), one sample every 0.25 λ_c is acquired. We know from the literature that the correlation distance in urban area is about 0.5 λ_c. Consequently, sampling at the Doppler sample rate will allow the collection of the maximum number of uncorrelated samples if the correlation distance (r) is reasonably close to 0.5 λ_c. If r becomes smaller than 0.5 λ_c, this rate allows collection of the maximum number of uncorrelated samples until $r < 0.25$ λ_c. If the correlation distance becomes larger than 0.5 λ_c, more correlated samples will be collected, but as long as the samples are averaged over 10 to 40 λ_c (4), the maximum number of correlated samples will be obtained. Using this sample rate and (4), we can determine the number of measurements (M) made when the channel is stationary, and also the number of uncorrelated samples collected.

Table 3. A channel sampling example for a carrier frequency of 5.75 GHz and a mobile velocity of 15 m/s. The Doppler sample-rate is 0.87 ms. The number of samples collected as the mobile travels 10 to 40 λ_c is M.

$f_d(Hz)$	$BW_d(Hz)$	$t_{bi}(ms)$	$M_{10\lambda_c}$	$M_{40\lambda_c}$
$\pm$287.5	575	0.87	40	160

Sampling at the Doppler BW rate for this mobile velocity and carrier frequency, we will acquire 40 to 160 power samples over a distance of 10 to 40 λ_c (Table 3). For an averaging distance of 20 λ_c, 80 samples will be collected. If the correlation distance is 0.5 λ_c, then this will result in 40 uncorrelated samples. This is a sufficient number of uncorrelated samples to achieve the desired accuracy in computation of the mean value of the received power. The vehicle speed is

used during processing to adjust the averaging interval so that (4) is honored. Since the probe collects 512 records or power samples per burst, the averaging interval at slower vehicle speeds can be lengthened by increasing the number of samples averaged up to 512 records. If the vehicle is moving too slowly to collect a reasonable number of uncorrelated samples in 512 records, the data burst is discarded. When the vehicle is moving near the average speed estimate, or up to twice as fast, multiple averages per data burst are computed so all the data in the burst is utilized.

The fast PN power readings allow measurement of deep fades while the Doppler sampling rate enables an accurate estimate of the mean power. If one samples the channel at less than the Doppler rate there will be two negative consequences. First, one may not be able to acquire a sufficient number of uncorrelated samples when the channel is stationary to accurately estimate the mean. Second, one will not be able to characterize the fast fading and time dynamics of the channel which are needed to predict receiver performance. A poor estimate of the mean power will also negatively impact the accuracy of slow fading data, its slope and its variance when computing a power law channel model.

The preceding examples illustrate how the Doppler sampling rule and PN probe configuration enable the time variability of the received power (fast fading) and the average power over a small region to be determined. The received power time series acquired in this fashion can now be characterized in terms of its probability density function (PDF). The PDF and the moments of the distribution can then be used to develop a statistical description of the radio channel. For link budget analysis, the basic transmission loss, which is the difference between the power at the transmit antenna terminal minus the power at the receive antenna terminal is also analyzed using the same statistical methods. As such, our analysis of received power sampling and statistics applies directly to basic transmission loss data which will be shown in Section 7.

6 SIGNAL PROCESSING

6.1 Processing Sequence

To process channel probe data is necessary to read parameters from data header files. These parameters include sampling rate, number of channels, channel frequencies, time between records, and number of records per data burst.

To allow processing to relevant data metrics, the header data also includes, transmitter power for each channel, transmitter and receiver antenna gains and patterns, transmitter and receiver GPS coordinates, channel bit rate, and the code sequence specifiers.

These data are relevant to a specific recording route or run where common statistics can be calculated and analyzed. After this information has been read from the header files and assembled, the data processing can begin. To simplify this section, we assume these relevant parameters are known and that we are not concerned with processing multiple channels. The details for de-interleaving the binary data from the data acquisition system is also skipped as they can be found in the digitizer user manuals.

We will start with a data record for one RF channel and proceed through the processing steps. Additional channels can then be processed in the same manner. The processing scheme is generalized to handle variable bit rates (BR) and knows specific parameters for each channel.

1. The file header data is read and stored.

2. A complete data is read. The binary record contains interleaved 16-bit integers representing the output of the ADC for all channels. The data is de-interleaved and then each burst of data consists of $(NImpulses)(NSamples\,per\,Impulse)$ of binary integers. This is the raw IF data for one channel.

3. If velocity = 0, we throw out the entire data burst because we will not be able to average the fast fading data and calculate slow fading. If this occurs we return to step 2 and read the next data burst.

4. Then the ADC data is converted to volts and system calibration is applied. The integer data has now been converted to volts and scaled so the received power can be calculated in watts (W).

5. The data is down-converted to baseband in preparation for the correlation processing needed to calculate R_{xy}.

6. Before R_{xy} is calculated, over-sampled data must be filtered and decimated to improve multi-rate processing speeds.

7. The averaging interval is calculated using carrier wavelength and vehicle speed while dividing the data burst into 2^n segments such that each segment spans an interval between 10 and 40 λ. This division ensures that all the CIRs in the burst are used.

8. Check records to be averaged. If any point has near A/D over-ranging (32,000 bits), discard the entire segment for averaging or all records in the segment for non-averaged data.

9. Calculate PDPs and average power delay profiles (APDPs).[6]

10. Calculate fast fading power data using PDPs and slow fading power using APDPs.

11. Determine the PDP's IOD_{Pk} and if minimum IOD_{Pk} requirement is met process for delay spread. Disregard data with an insufficient number of samples for delay spread averaging.

12. Filter noise from CIR for power processing.

13. Calculate power by summing PDPs and APDPs to determine the total received power. If enabled, sum power at multiple bandwidths.

14. Use average power and non-averaged power and transmitter power to calculate basic transmission loss.

15. Calculate excess loss (difference between basic transmission loss and free space loss).

16. Determine K factors (defined in section 7.1) if desired from non-averaged power data.

17. Store all data indexed to GPS coordinates and transmitter-receiver separation.

Several steps in this sequence are given in more detail in the following sections.

6.2 IF Processing

6.2.1 ADC Voltage

The system power calibration constant is measured in the laboratory using the setup shown in Figure 10 and a wideband power meter. In this configuration, the PN sequence is being transmitted at RF. The same cables that will be used to connect the transmitter and receiver antennas in the field are used in the laboratory so their losses are included in the calibration. The additional information needed to calculate transmitted and received power from measurement data are the antenna gains and the transmitter power for each channel. These are either determined from the manufacturer's specifications or measured in the field.

Then the n^{th} ADC sample, x_n, is converted to volts by scaling it by the ADC calibration constant C_{ADC} which has units of volts/bit (V/b). It is somewhat unnecessary to scale the digitizer bits into volts because this can be included in the system calibration constant. Nevertheless, it is sometimes useful to examine raw data values in volts. The scaled ADC voltage is named VIF_n.

$$VIF_n = x_n C_{ADC} \tag{5}$$

[6]Some authors define the PDP as the expected value (with respect to t) of $|h(t,\tau)|^2$. In this report we refer to this expected value as the APDP in order to distinguish this from the PDP measured at a specific time.

6.2.2 System Calibration Constant

If the processing sequence is in calibration mode, the program proceeds with signal down-conversion and correlation processing so a calibration constant can be calculated. If field data is being processed the system calibration factor (CF) is applied to the raw data here as another linear factor and then the down-conversion and calibration processing continues. The field processing sequence will be illustrated and the calibration factor calculation will be given later. In field processing mode,

$$IF_n = (VIF_n)(CF) \tag{6}$$

6.2.3 Down-Conversion

The calibrated IF_n signal is now down-converted to baseband and decimated and filtered if needed if the IF time series has been over sampled. The calibrated and down-converted time series is xb_n. The down-conversion process consists of two steps. The IF_n time series, x_n is down-converted to base band, and then it is low-pass filtered. The down-conversion process is

$$xb_n = IF_n e^{-i\omega_c t_n}, \text{ where } \omega_c t_n = n\pi/2. \tag{7}$$

In these equations, ω_c is the IF frequency in radians/sec, $t_n = n\Delta t$, $\Delta t = 1/f_s$, $f_s =$ sample rate with $f_s = 4CR$.

6.3 Baseband Processing

6.3.1 Correlation Processing

A discrete Fourier transform (DFT) is used to transform the baseband time series into the frequency domain where it is low-pass filtered. The filtering is a necessary part of down-conversion. The filter is the standard rectangular function where

$$rect(n) = \begin{cases} 1 & \text{for } -1/2 < n < 1/2 \\ 0 & \text{elsewhere.} \end{cases}$$

The data are in complex baseband format and ready for correlation processing. Correlation in the frequency domain is accomplished by element-wise multiplication of the baseband series with the DFT of the transmitted signal $pn(t)$. The output is an approximation of the complex impulse response of the channel (R_{xy}), which is also referred to as CIR in the text. Bold is used to represent frequency domain sequences npn points long. If the DFT of $pn(t)$ and $rect(n)$ are indexed from $-npn/2$ to $npn/2$,

$$\mathbf{IF'}_n = \mathbf{rect}(2n/npn)\mathbf{XB}_n \tag{8}$$

$$\mathbf{R}_{xy} = (\mathbf{IF'}_n)(\mathbf{PN}_n)\,. \tag{9}$$

6.3.2 Average Power Delay Profile

The first step in using the complex impulse response (CIR) is to calculate the PDP. Using R_{xy} to represent the CIR,

$$PDP = \left| R_{xy} \right|^2 \tag{10}$$

The PDPs are averaged before the slow fading power and delay-spread calculations and are now designated as APDPs.

$$APDP = \frac{1}{N} \sum_{n=1}^{N} PDP_n \tag{11}$$

The vehicle speed and carrier frequency are used to determine N, the number of PDPs to average so as not to exceed a distance of 10 to 40 λ (4) with $t_s = N * t_{bi}$.

6.3.3 Delay Spread

The interval of discrimination, which is the peak to tail ratio of the APDP in dB, is then checked to see if the APDP is valid and can be used for the delay spread calculation. We require an IOD_{Pk} of 23 dB. We compute IOD_{Pk} using the last 10% of the APDP where no multipath is expected due to the long delay times. If this requirement is met, APDP data more than 20 dB below the correlation peak are set to zero and the mean delay (d) and delay spread (S) are calculated using (12) and (13).

$$d = \sum_{k=1}^{NPN} \tau_k APDP(\tau_k) / \sum_{k=1}^{NPN} APDP(\tau_k) \tag{12}$$

$$S = \left[\sum_{k=1}^{NPN} (\tau_k - d)^2 APDP(\tau_k) / \sum_{k=1}^{NPN} APDP(\tau_k) \right]^{1/2} \tag{13}$$

6.3.4 Received Power

The non-averaged received power is calculated by summing PDPs which have been scaled by the calibration factor.

$$P_i = \sum_{k=1}^{NPN} PDP_k \tag{14}$$

The slow fading received power component is calculated by summing an APDP.

$$P_s = \sum_{k=1}^{NPN} APDP_k \tag{15}$$

6.4 Calibration Constant

The calibration factor (CF) is calculated using the measured input power (P_{in}) and a PDP calculated in the back-to-back configuration as shown in Figure 10.

We measure P_{in} using a power meter at the receiver antenna port. The variable attenuator is used to adjust the transmit power so it is within the receiver's dynamic range. A group of 8 data bursts are collected on each receiver channel. The first burst is at the maximum signal input of the receiver and each subsequent burst is attenuated by 10 dB until the signal is in the receiver noise. A calibration constant is then calculated by averaging over the linear portion of the receiver's calibration curve (Figure 11).

In calibration mode, the recorded times series x_n is scaled by the digitizer C_{ADC}. This IF signal is then down converted and R_{xy} and its corresponding PDP are computed. The CF is then averaged over a burst of data and over the digitizer linear range where N_B is the number of bursts averaged, N_i is the number of impulses or PDPs per burst and the CF is

$$CF = \frac{1}{N_i N_B} \sum_{i}^{N_B} \sum_{j}^{N_i} \sum_{k}^{NPN} PDP_{ijk}/P_{in}. \tag{16}$$

Figure 11 is a typical 4 channel plot of calibration data. The input power to the receiver was approximately -35 dBm to -105 dBm $\pm$ 0.2 dB. These levels were set using precision variable attenuators with 10 dB steps. From this plot we see the linear range of the calibration factor is between bursts 1 and 6.

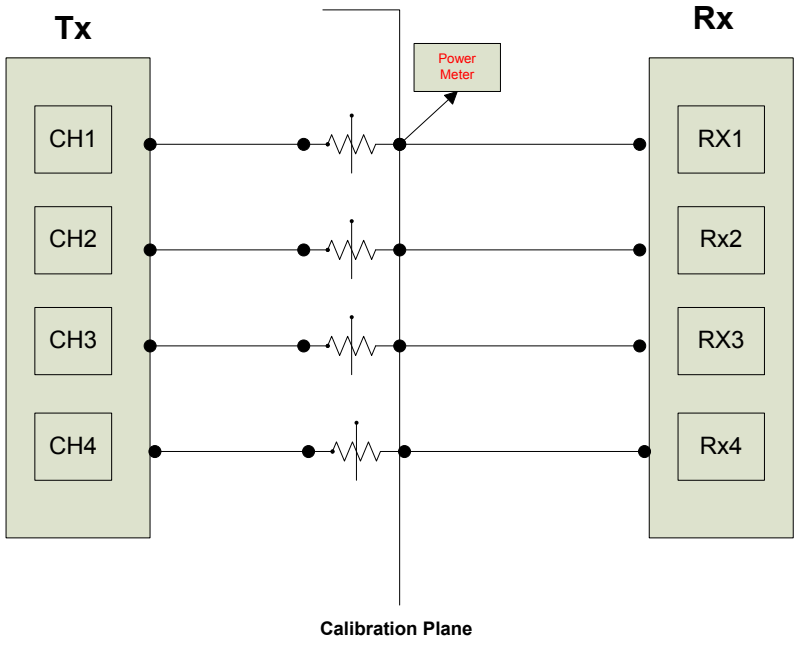

Figure 10. Block diagram for a channel sounder power calibration in back-to-back configuration.

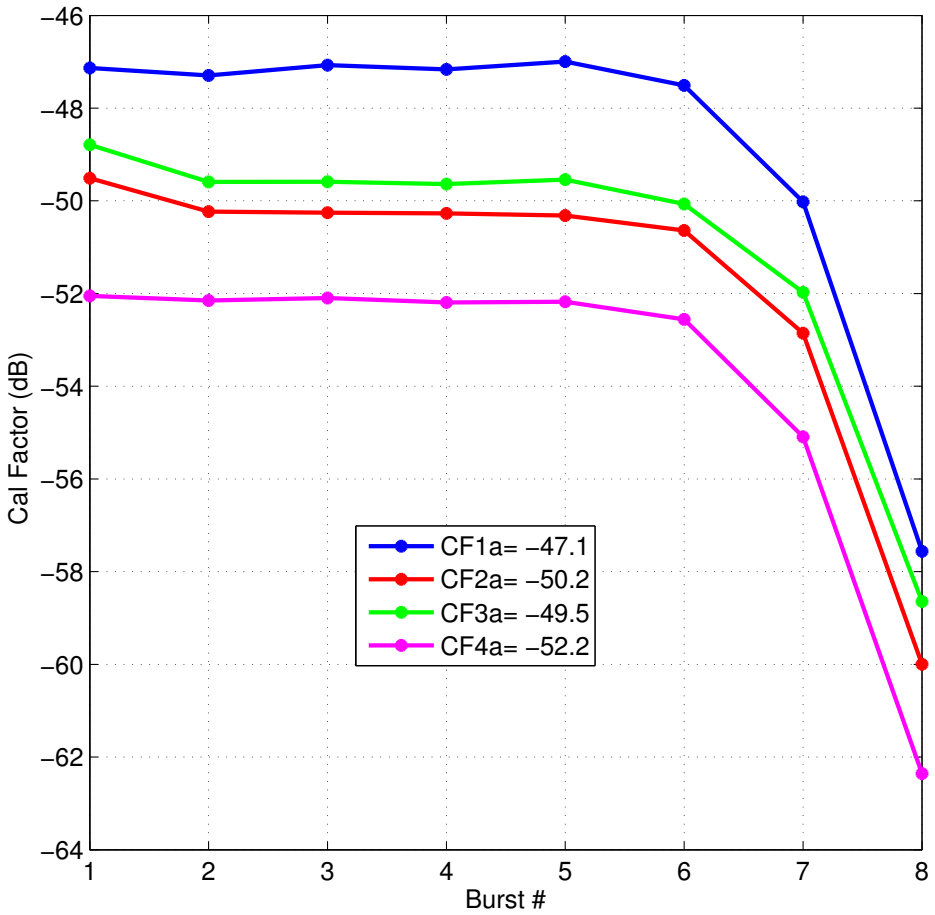

Figure 11. Average calibration factors for a multi-rate receiver. Channels: Ch1, 183 MHz, 2 Mb/s; Ch2, 915 MHz, 10 Mb/s; Ch3, 1602.5 MHz, 5 Mb/s; Ch4, 5750 MHz, 10 Mb/s.

7 CHANNEL MODEL DEVELOPMENT

There are multiple methods for using channel sounder impulse response data. In all cases, the data should be collected in or near the frequency band of the proposed system, using similar antennas and in similar geographic settings.

One method is to use the impulse response to model the performance of a specific radio receiver. In this case, the impulse response is used to calculate the receiver input $z(t)$, by convolution with the baseband representation of the bandpass transmitter waveform $u(t)$:

$$z(t) = \int_{-\infty}^{\infty} h(t,\tau)u(t-\tau)d\tau, \tag{17}$$

where $h(t,\tau)$ is the channel impulse response at time t due to an impulse at time $t-\tau$.

Another use of impulse data is the development of channel models for receiver compliance testing. These models are included in the physical layer of mobile radio standards. The models are usually tapped delay line models which can be implemented in hardware to test receivers. The impulse data is used to specify tap weights, delays and tap statistics.

A third possibility is to use the impulse data to develop a statistical model of the mobile radio channel. This model can be used for link budget or interference analysis. For these cases we would like a simpler model of the channel than its time varying impulse response $h(t,\tau)$. For link budget and interference calculations this can be the average received power versus transmitter-receiver separation and its variance. This model has three components:

1. Fast fading signal and its time variability

2. Slow fading data calculated by averaging fast fading data

3. The average propagation-path loss calculated using linear regression and the variance of the slow fading data about this average value

7.1 Fast Fading Statistics

We have shown how the digitized waveform or voltage at the antenna terminals is used to compute the radio channel impulse response $h(t,\tau)$ from R_{xy}. It has also been shown how the impulse data is processed to yield received power in watts (w) from this digitized waveform data. To further develop the path-loss model, it is necessary to understand the statistical description of the fast fading waveform.

Two statistical distributions are commonly used to model fast fading *even though the assumptions of these statistical models don't apply to all radio channels*. These are the Rayleigh and the Nakagami-Rice distributions.

The Rayleigh distribution is used to describe narrowband fading in urban areas. In this environment there is no direct path signal and received signals are multipath signals with a uniform phase distribution.

At baseband, the envelop voltage $z(t)$ seen by a radio receiver is,

$$z(t) = \sqrt{i(t)^2 + q(t)^2}, \tag{18}$$

where *i(t)* is the in-phase receiver voltage waveform, and *q(t)* is the quadrature receiver voltage waveform. The PDF of the envelope voltage is

$$p(z) = \frac{z}{\sigma^2} e^{-z^2/2\sigma^2}, \tag{19}$$

which is known as the Rayleigh PDF. The term σ^2 is equal to the mean power of the process and $z^2/2$ is the instantaneous signal power.

The cumulative distribution function (CDF) of this PDF gives the probability that the envelope function of the random variable Z does not exceed the value z. Here random variables are denoted using capital letters and the values they can take by lower-case letters. Also, CDFs are denoted using upper case letters and PDFs by lower case letters.

$$Prob\{Z \geq z\} = P_Z(z) = 1 - e^{-z^2/2\sigma^2} \tag{20}$$

For simplicity we will use Hufford's nomenclature (from his notes on Statistical Distributions [18]). Let w_0 and w represent the mean and instantaneous received power. Substituting, the CDF of the fast fading power data becomes

$$Prob\{W \geq w\} = P_W(w) = 1 - e^{-w/w_0} \quad (w \geq 0). \tag{21}$$

For plotting purposes, we are more concerned with the complementary CDFs (CCDF), where both the signal power and probability are increasing functions. The CCDF is

$$Prob\{W \leq w\} = e^{-w/w_0}. \tag{22}$$

In the more general case, both direct path and multipath signals can arrive at the receiver. The distribution of the envelope voltages in this case can be described using Nakagami-Rice (Rician) statistics.

If z_i and z_q represent the in-phase and quadrature components of the received signal, and $\bar{z_i}\,(\bar{z_q})$ are the average value of $z_i\,(z_q)$, then $s^2 = (\bar{z_i})^2 + (\bar{z_q})^2$ and the envelope voltage is $z = \sqrt{z_i^2 + z_q^2}$. The PDF of this distribution is

$$p_{Rice}(z) = \frac{z}{\sigma^2} e^{-(z^2+s^2)/2\sigma^2} I_0\left(\frac{zs}{\sigma^2}\right) \tag{23}$$

where s^2 is the power in the direct signal, σ^2 is the variance of z, $2\sigma^2$ is the scattered or indirect power, and I_0 is the modified Bessel function of order 0 and $s^2/2\sigma^2$ and is called the Rician K-factor.

$$p_{Rice}(z) = \frac{z}{\sigma^2} e^{-z^2/2\sigma^2} e^{-K} I_0\left(\frac{z}{\sigma}\sqrt{2K}\right) \tag{24}$$

The ratio of the received power in the direct path to the total power in the scattered or multipath signals is represented by K. When there is no direct path, $K = 0$, $e^{-K} = 1$ and $I_o = 1$ yielding the worst case Rayleigh PDF. When there is no scattered power $K = \infty$. This corresponds to a constant amplitude signal. The CCDF of the Rician distribution is

$$P(z)_{Rice} = e^{-(K+z^2/2\sigma^2)} \sum_{m=0}^{\infty} \left(\frac{\sigma\sqrt{2K}}{z}\right)^m I_m\left(\frac{\sqrt{2K}}{\sigma}\right) \tag{25}$$

For analysis of the fast power fading, we would like to plot data on Rayleigh probability paper in decibels. Using this paper will ensure that a Rayleigh distribution will plot as a straight line. We note that power in decibels is $W = D\,ln\,w$ where $D = 10\,log_{10}\,e = 4.3429$, Hufford [18]. Using Hufford's method the ordinate scale for Rayleigh paper is

$$x = -D\,ln\,ln\frac{1}{P_w}. \tag{26}$$

If we allow P_w to vary from 0.1% to 99.9%, then x varies from -8.39 to 30.00. On this paper the Raleigh distribution plots as a straight line. If we have a 50 dB range on the ordinate we will obtain a slope of -1 if we make the graph 1.3 times as high as it is wide. Similar scales can be developed for different ordinate and abscissa ranges.

The Rician distribution can also be plotted on Rayleigh paper as in Figure 12. This plot illustrates the large range of probable power levels for distributions between Rayleigh scattering ($K = -\infty$ in dB) and distributions with large K values, indicating a strong direct signal as well as small scattered signals. These distributions are plotted relative to the median for different K values. We see that the scattered power signals, described using the Rayleigh distribution, experience 18 dB or more fading about 1% of the time. When the ratio of direct to scattered power equals 100 (K = 20 dB), a 2 dB or more fade is predicted 1% of the time.

Examples of non-averaged power data are shown in Figure 13. These data were collected using the PN sounding method at a carrier frequency of 430 MHz in a Superior, CO mall parking lot. Using the vehicle velocity from the GPS, the time series data was plotted versus distance traversed in wavelengths at the carrier frequency.

These four data records correspond to the time series used to compute the first four average power points (smallest r) in Figure 17. The average value in watts of these time series equals the power level of the slow fading data points plotted on Figure 17. The CCDF of the second time series from the top shown on Figure 13, is plotted on Rayleigh paper in Figure 14. We also see that its distribution plots almost as a straight line, indicating that it can be described using the Rician

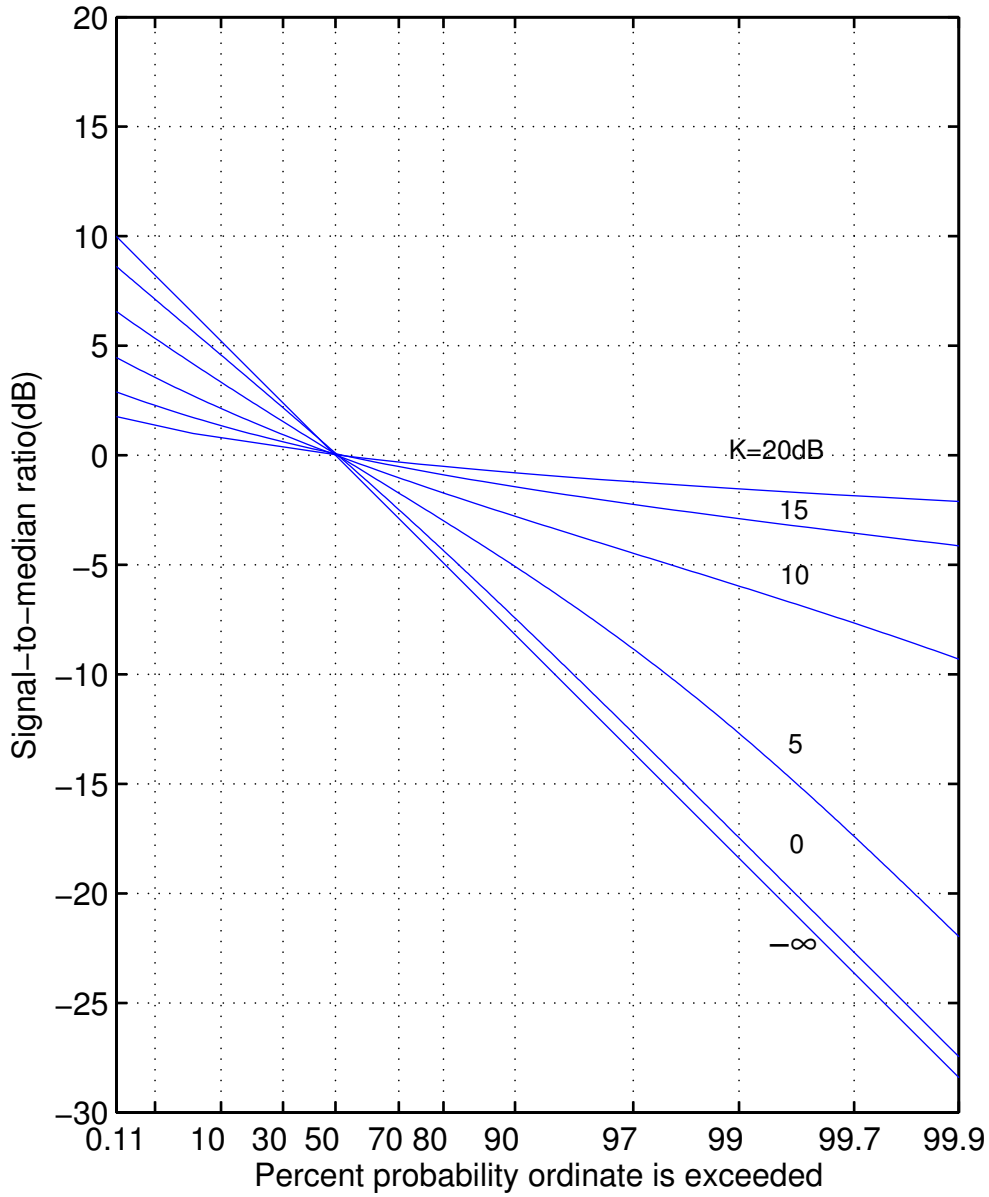

Figure 12. Examples of the Nakagami-Rice distribution drawn on Rayleigh probability paper. The value of K is the ratio (in decibels) of the constant power to the scattered. When $K = -\infty$ there is no constant signal and the distribution is Rayleigh.

distribution. We can estimate the data K factor from the graph as well and see it is between 15 and 20 dB, indicating a strong direct component between 30 to 100 times larger than the scattered signal component. The top time series from Figure 13 is also plotted on Rayleigh paper in Figure 15. Here we see the K factor can be estimated to be about 10 dB. This correlates well with the time series, as we can see from Figure 13 that this time series is more variable, indicating more scattered signal components. But K is still large and indicates that the direct signal power is about 10 times the scattered signal power.

These examples demonstrate how the Rician distribution can be used to model fast fading in a wideband channel. However, it should be recognized that the nature of fading is bandwidth-dependent, with larger bandwidths resulting in less fading due to integrating frequency-dependent channel power over a range of frequencies. The effects of the measurement bandwidth on the probability of fading have been analyzed by Wilson [19].

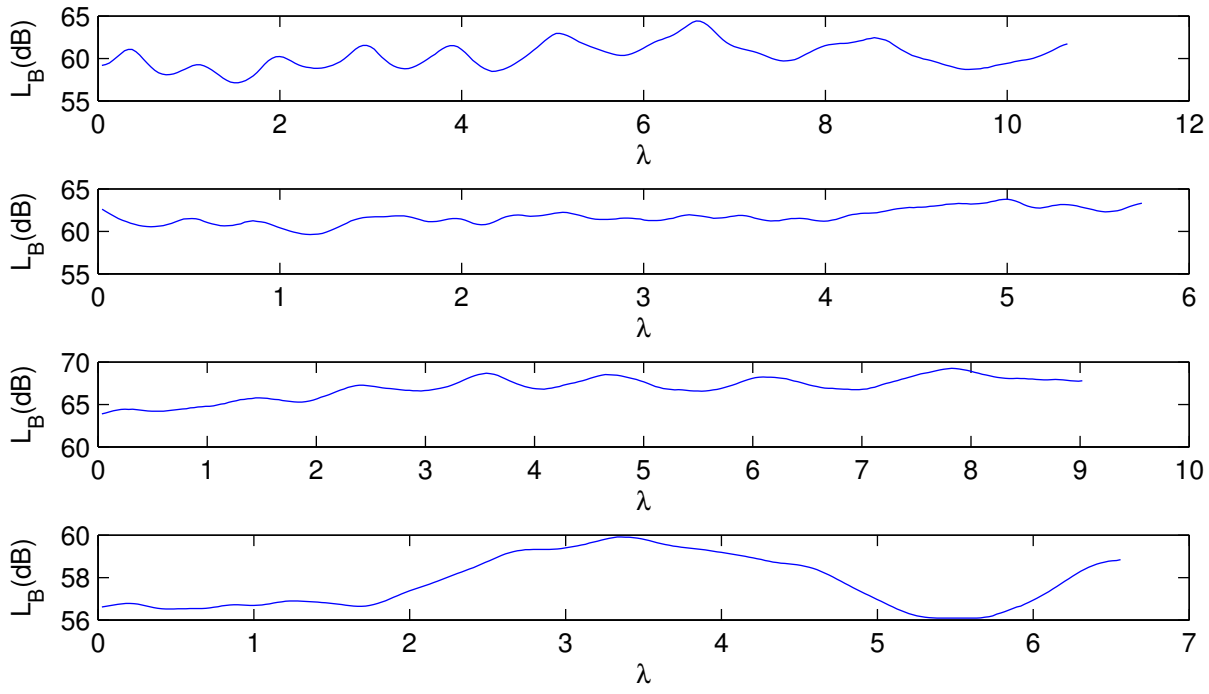

Figure 13. Fast fading data used to calculate the first 4 points of slow fading average power estimates on Figure 17. Data represents line of sight at small transmitter receiver separation. Proceeding from top graph to bottom graph mean value estimates for basic transmission loss (L_b) are $\mu =$ 60.3, 61.7, 67.0, and 57.8 dB. The mobile speed for these data are 5.8, 3.1, 4.9 and 3.6 m/s.

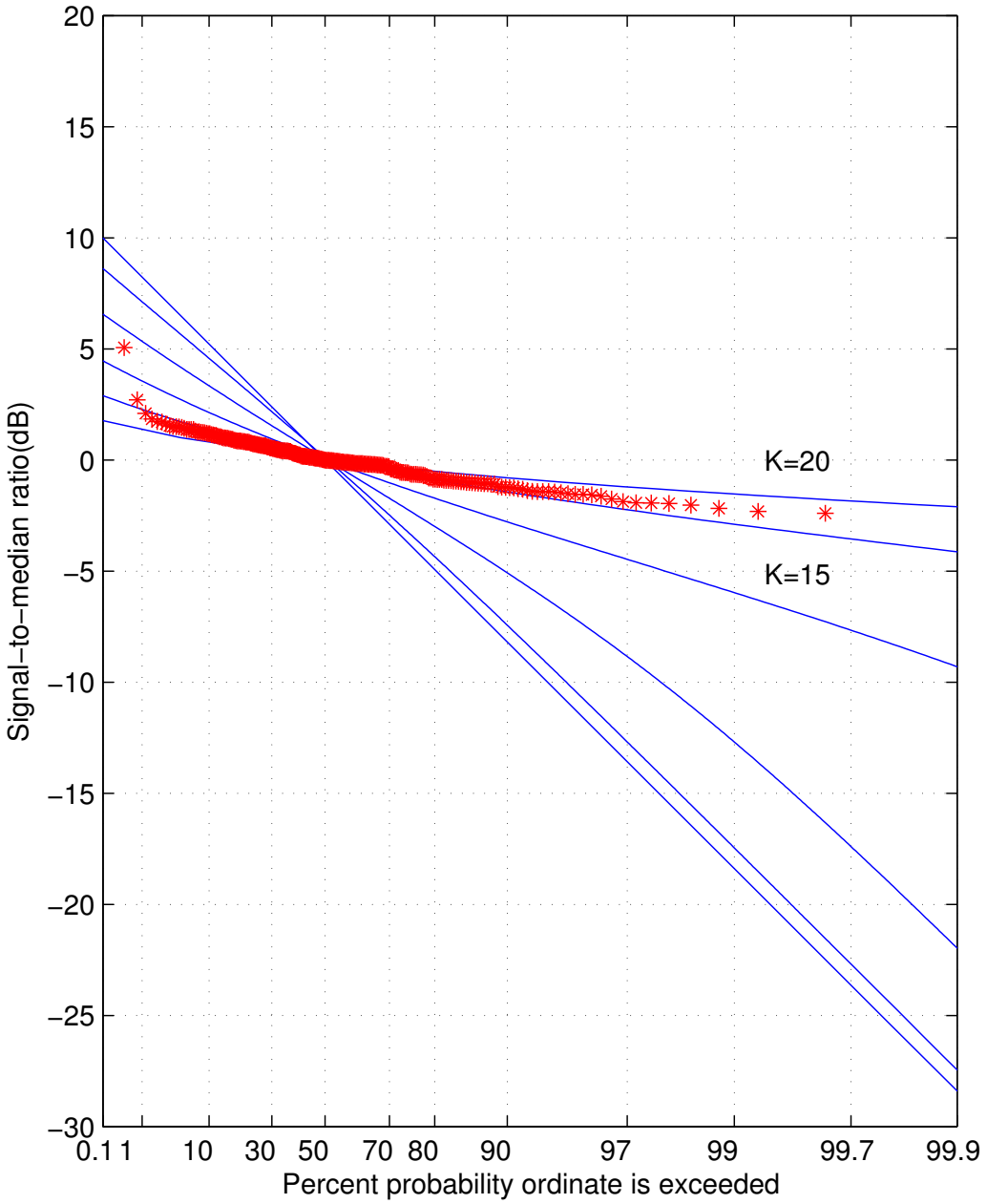

Figure 14. Fast fading data from record 2 (second record from top on Figure 13) plotted on Rayleigh paper. Data represents line-of-sight at small transmitter receiver separation. The data is approximately Rician with K between 15 and 20 dB indicating a strong direct signal component.

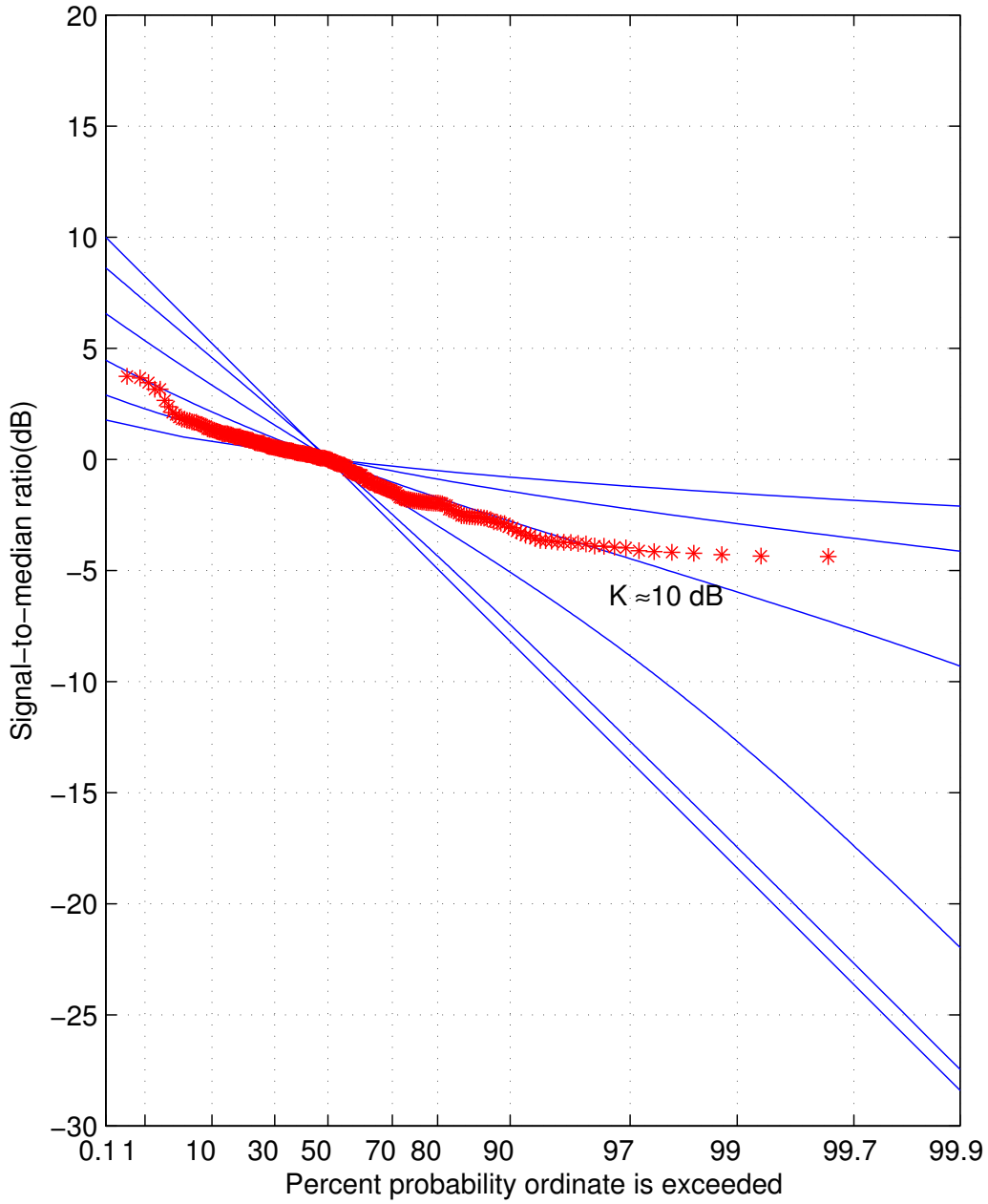

Figure 15. Fast fading data from record 1 (top of Figure 13) plotted on Rayleigh paper. Data is line-of-sight at small transmitter receiver separation. The data is approximately Rician with $K \approx 10$ dB indicating a strong direct signal component but with more scattered signal power than record 2 (Figure 14

.

7.2 Slow Fading Statistics

The log-normal distribution is often used to describe long-term or large-scale variability of the received power. In our case this is the more slowly-varying mean power calculated from the fast fading data. This large-scale variability is due to changes in the scattering environment as the mobile unit moves through an area. This could mean a group or cluster of buildings responsible for the multipath signals has changed. This causes the mean signal level to change as obstructions are removed or encountered on the mobile path. The well known PDF of the normal distribution is

$$p(x;\mu,\sigma^2) = \frac{1}{\sqrt{2\pi\sigma^2}} e^{-(x-\mu)^2/(2\sigma^2)} = \frac{1}{\sigma} n\left(\frac{x-\mu}{\sigma}\right), \tag{27}$$

where σ^2 is the variance and $\mu = E\{x\}$ is the mean of $p(x)$. The density of the "standard normal" distribution is $n(x) = (2\pi)^{-1/2} e^{-x^2/2}$ with $\mu = 0$ and $\sigma = 1$. The CDF of the standard normal distribution is

$$\Phi(z) = \int_{-\infty}^{z} n(x)dx = \frac{1}{\sqrt{2\pi}} \int_{-\infty}^{z} e^{-x^2/2} dx. \tag{28}$$

We evaluate $\Phi(z)$ using erf, the error function. The standard normal is then

$$\Phi(z) = \frac{1}{2}\left[1 + erf\left(\frac{z}{\sqrt{2}}\right)\right]. \tag{29}$$

The inverse of the CDF can be computed using the inverse erf

$$\Phi^{-1}(z) = \sqrt{2}\, erf^{-1}(2z-1), z \in (0,1). \tag{30}$$

To plot these CDF data we will use "normal" probability paper. To compute the axes for this paper we will need the complementary CDF,

$$Q(z) = \int_{z}^{\infty} n(x)dx = 1 - \Phi(z). \tag{31}$$

Using $n(z)$ and $Q(z)$ and upper case W for the decibel value of power, the complementary log normal CDF is

$$Prob\{W < z\} = Q\left(\frac{W - W_0}{\sigma}\right), \tag{32}$$

and the PDF is,

$$p(W) = \frac{1}{\sigma} n\left(\frac{W - W_0}{\sigma}\right), \tag{33}$$

where W_0 and σ are the mean and standard deviation of the decibel measures. We compute Q using the erf function,

$$P(W;W_0,\sigma) = Q\left(\frac{(W - W_0)}{\sigma}\right) = \frac{1}{2}\left[1 - erf\left(\frac{W - W_0}{\sigma\sqrt{2}}\right)\right] \tag{34}$$

The inverse of the Q is,

$$Q^{-1}\left(\frac{W-W_0}{\sigma}\right) = \mu + \sigma\sqrt{2}erf^{-1}(2W-1). \tag{35}$$

To construct log normal paper we would like the standard normal deviate Q to plot as a straight line with a slope of -1. We assign values to the abscissa (x) or probability axis so that

$$x = -Q^{-1}. \tag{36}$$

Equation (35) is used to determine x, but the x axis of the plot is labeled using the probability values of x. Figure 16 shows log normal distributions with variable σ plotted in this manner. We see that when σ becomes large the probability of signals above or below the median value increases rapidly. For instance for $P = 99.999$ and $\sigma = 1$, $W = -4$ dB while when $\sigma = 10$, $W = -42$ dB.

To compare our data to the standard normal deviate, we compute its residual by subtracting the mean value and use $\sigma = 1$ for a reference graph. The inverse of Q for plotting the residual data is then

$$P(W) = Q^{-1}(W) = \sqrt{2}erf^{-1}(2W-1). \tag{37}$$

A slow fading data set is plotted on Figure 17. Its distribution function plotted on log normal paper is shown on Figure 18. This data was recorded in a suburban shopping mall using the PN sounder with a carrier frequency of 430 MHz. The slow fading data has a $\sigma = 2.44$ relative to its best fit slope. These plotted data are residual values. Residual values represent the difference between the average value predicted by the best fit slope line and the individual slow fading data points. We can see the data residual is log normally distributed because it plots as a straight line on log normal paper. We see that the predominant slope of the residuals in Figure 18 falls between the $\sigma = 2$ and $\sigma = 3$ lines on the log-normal plot. This corresponds well with $\sigma = 2.4$ calculated using the individual data points and the best-fit line in Figure 17.[7]

In contrast to the fast fading which is bandwidth dependent, the slow fading is expected to be independent of bandwidth. This is because the slow fading is determined by averaging over the frequency-dependent fast fading due to multipath. In fact, the path loss data when measured with either a wideband (250 MHz) PN probe or a CW measurement system are equivalent when averaged over a few wavelengths [20],[21].

[7] Averaging intervals between 10 and 40 λ have been chosen for this data, which was collected at multiple frequencies simultaneously. This is a tradeoff between sampling fast enough to meet the Doppler criteria at higher frequencies and long enough to cover a sufficient number of wavelengths for the lower frequencies at reasonable vehicle velocities. The required channel sample rate for the higher frequency carriers, combined with burst durations of up to 1.5 s, yield between 16 and 512 power samples for averaging. If more than 64 uncorrelated power samples are acquired in one burst, multiple averages are calculated. When the mobile velocity and carrier frequency allow, 32 to 64 samples are selected for averaging over a distance between 10 and 20 wavelengths.

7.3 Power Law Channel Model

The signals and their statistics used to determine a power law channel model were demonstrated using impulse response field data in the previous section. To summarize, the components of the model are:

1. Expected value and variance of the fast fading waveform data for small areas. Distances are measured in wavelengths at the carrier frequency. These data are fast fading statistics.
2. Expected value and variance over larger distances measured radially from the transmitter site. These data are slow fading statistics.

For link budget application, one needs the probability of exceedance for basic transmission loss (L_b) which includes:

1. The average value of the slow fading.
2. The exceedance probability of the slow fading residual.
3. The exceedance probability of the fast fading residual.

The statistical parameters (μ, σ) used to estimate basic transmission loss (L_b) can also be used to estimate the received signal strength (S) for a mobile as well as the signal strength of an interfering signal (I). It has been found that the joint distribution of these two signals (S, I) is also log normally distributed and can be used to estimate the co-channel signal to interference ratio (S/I) [22]. This model is very sensitive to the average path loss and its variance. To determine S/I it important that these parameters be estimated accurately. Errors in estimation of these statistics will be discussed further in a follow on report.

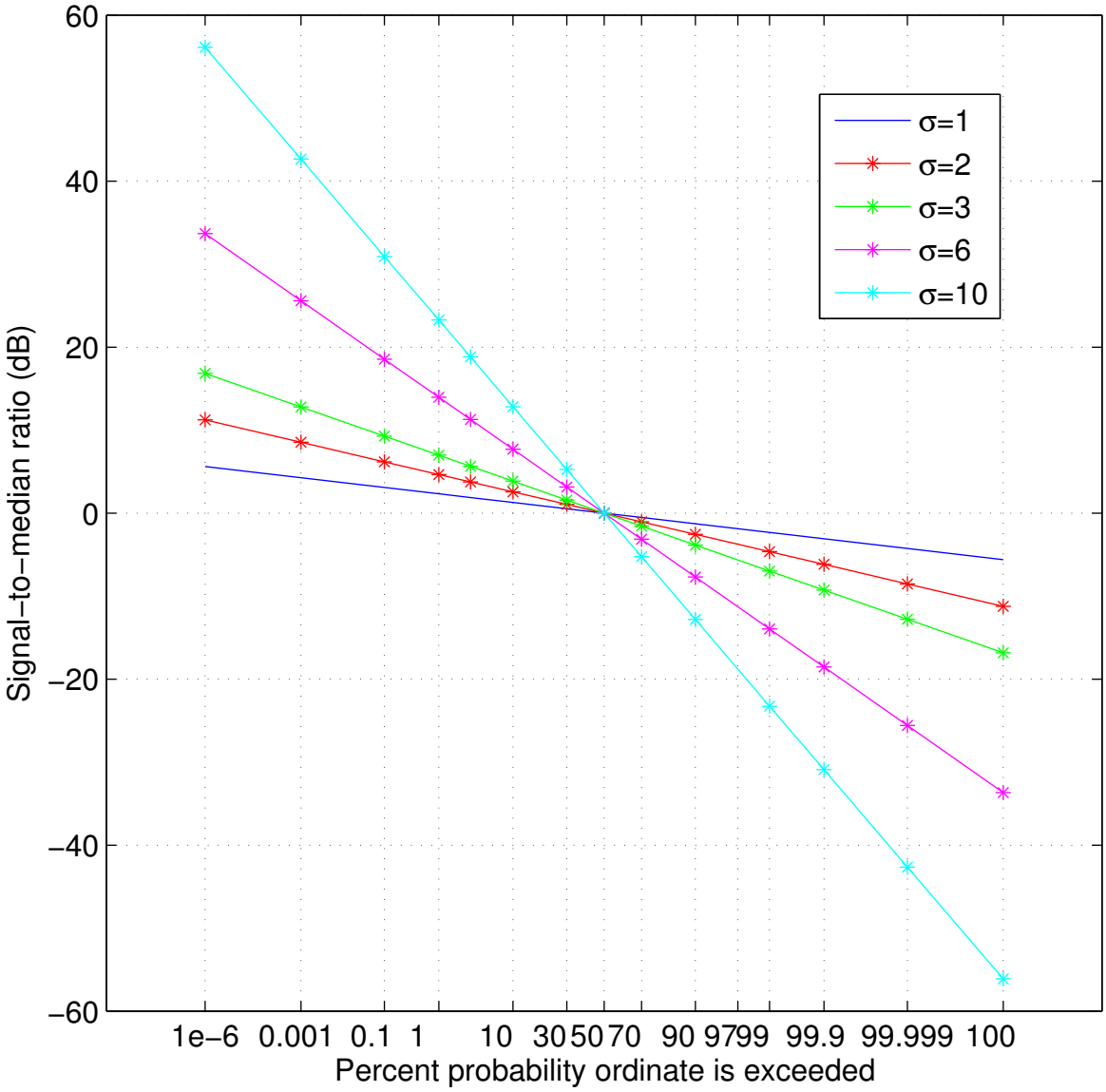

Figure 16. Log normal distributions with $\sigma = 1, 2, 3, 6, 10$ plotted on normal paper.

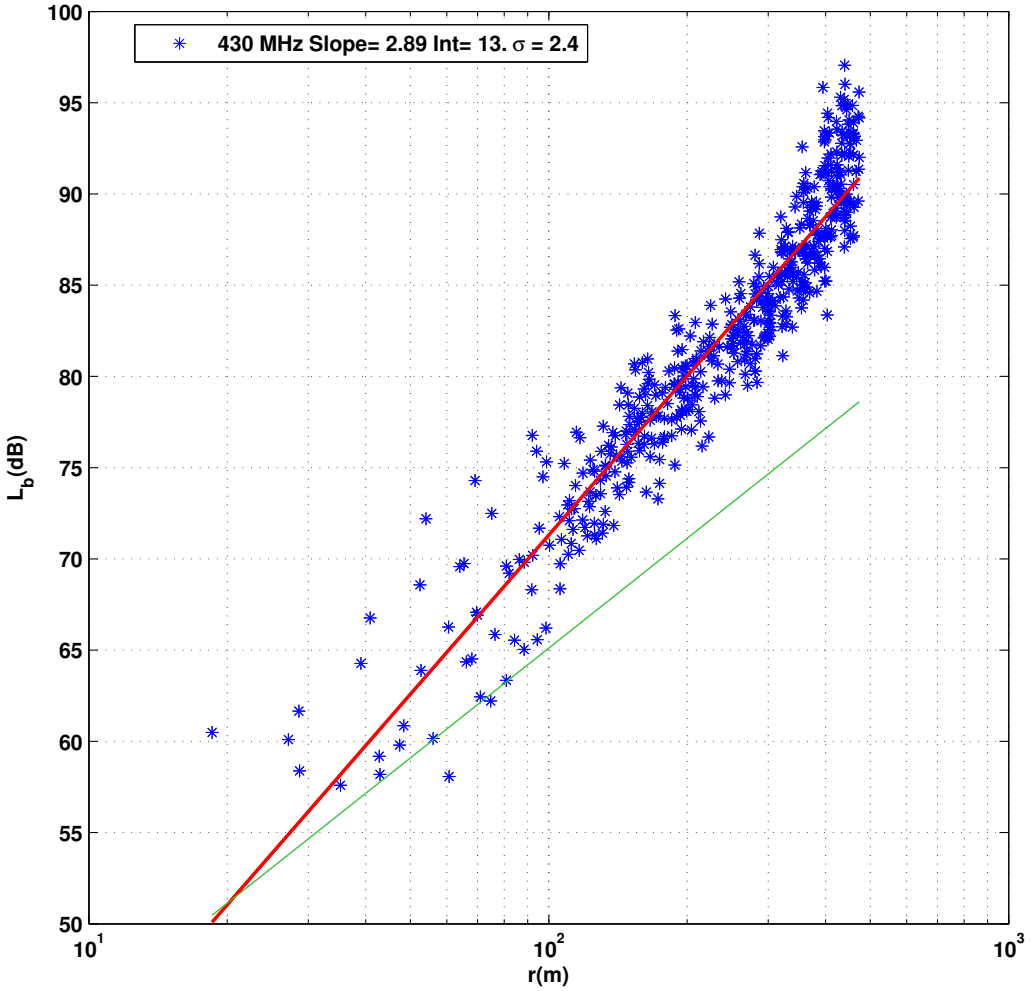

Figure 17. Slow fading data (blue stars) measured at 430 MHz in Superior Colorado. A best-fit line (red) is used to determine the average path loss slope. This slope is 2.9 and the slow fading distribution has a $\sigma = 2.4$ about the mean slope line. The free-space loss is plotted for reference (green).

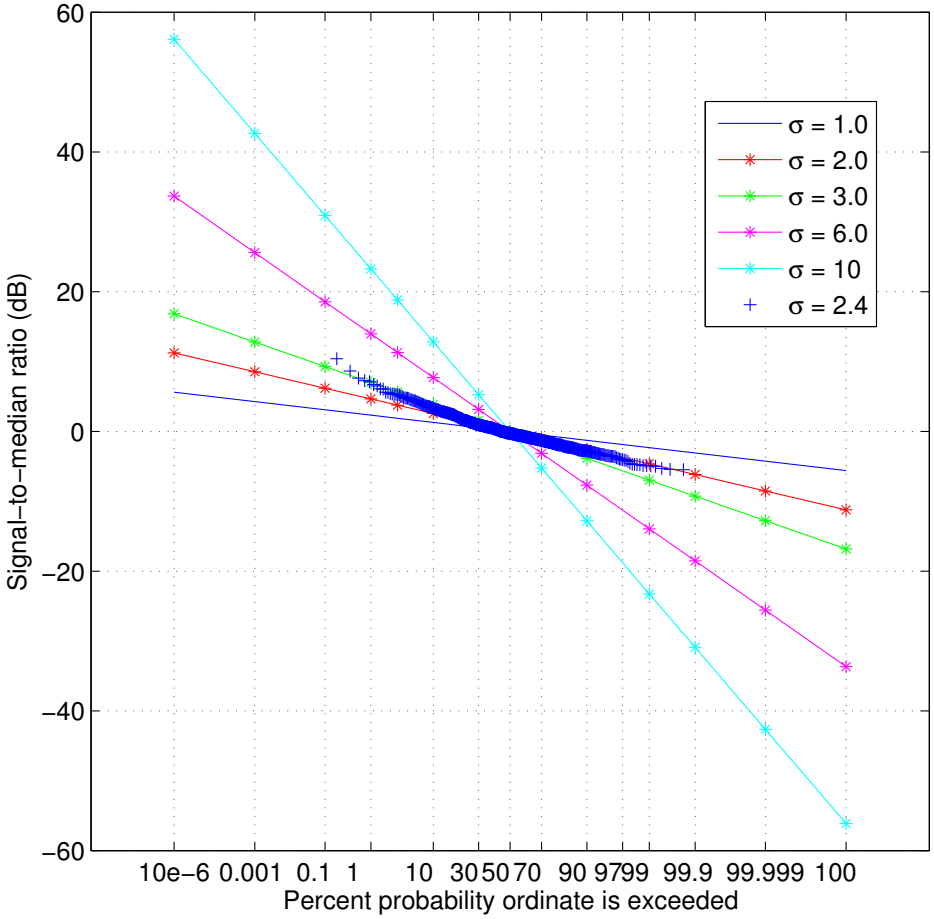

Figure 18. The slow fading power data distribution at 430 MHz data from Figure 17. The CCDF (complementary cumulative distribution) is plotted on log normal paper relative to zero mean log normal distributions with a range of σ values. The measured data are indicated by blue plus symbols. The straight line of the measured data indicates that the distribution is log normal with a σ between 2 and 3. The value of σ calculated from the data is $= 2.4$. Data were measured using the PN impulse response system.

8 CONCLUSIONS

This report provides a description of radio channel impulse response probe design, measurement methods, data processing methods, and mobile channel statistics, as well as an example of channel modeling using impulse data.

Important conclusions that can be inferred from this report are:

1. Channel measurements are based on a linear channel model with an impulse response and additive noise.

2. The impulse response can be approximated using correlation processing.

3. The PN sequence provides an impulse-like autocorrelation function which is well suited for channel sounding.

4. The PN sequence has several properties which make it a good choice for channel measurements. They include processing gain, the ability to vary measurement BW and orthogonality when necessary for multiple channel or antenna operations at the same frequency.

5. The wideband nature of the PN sequence is necessary when modeling digital systems because it can be used to measure the dispersive nature of the radio channel.

6. It is important to measure the waveform seen by the receiver if one wants to predict the performance of radio systems using measurement data.

7. The minimum sampling requirements for the receiver waveform can be determined using the Doppler equation, the carrier frequency, and the vehicle velocity.

8. The mobile radio channel is not stationary. The stationarity interval for fast fading is variable in different geographic locales. It has been estimated to be a few tens of carrier wavelengths in urban areas.

9. Without properly sampling the waveform data at the Doppler rate, the statistics (mean value and its variance) needed for a power law channel model cannot be accurately determined. This is because the channel is only stationary for a few tens of wavelengths and the mobile has limited time (distance) to collect the required number of uncorrelated samples needed for an accurate estimate of the mean.

9 REFERENCES

[1] G. Turin, F. Clapp, T. Johnson, S. Fine, and D. Lavry, "A statistical model of urban multipath propagation," *IEEE Trans. Vehicular Tech.*, VT-21, pp. 1-11, Feb. 1972.

[2] D. Cox, "Delay doppler characteristics of multipath propagation at 910 MHz in a suburban mobile environment," *IEEE Trans. Antennas and Propagation*, AP-20, pp. 625-634, Sep. 1972.

[3] R.W. Hubbard,"Characteristics and applications of a PN channel probe," OT Technical Memorandum 76-218, May 1976.

[4] R.F. Linfield, R.W. Hubbard, and L.E. Pratt, "Transmission channel characteristion by impulse response measurements," OT Report 76-96, Aug. 1976.

[5] G.A. Hufford, R.W. Hubbard, L.E. Pratt, J.E. Adams, S.J. Paulson, and P.F. Sass, "Wideband propagation measurments in the presence of forests," CECOM R&D Tech. Report 82-CS029-F (NTIS Order No. AD-113698), Jan. 1982.

[6] J.A. Wepman, J.R. Hoffman, L.H. Loew, and V.S. Lawrence, "Comparison of wideband propagation in the 902-928 and 1850-1990 MHz bands in various microcellular environments," NTIA Report 93-299, Sep. 1993.

[7] K.C. Allen and Lindsay-Stewart, "Method and apparatus for measuring the impulse response of a radio channel," U.S. Patent Number 5,371,760, Dec. 1994.

[8] Robert C. Dixon, *Spread Spectruum Systems and Applications*, New York, John Wiley and Sons, 1994, p. 64.

[9] Roger L. Peterson, *Digital Communications and Spread Spectruum Systems*, New York, Macmillan, 1985, p. 385.

[10] P. Papazian, Y. Lo, J. Lemmon, and M. Gans, "Measurements of channel transfer functions and capacity calculations for a 16x16 BLAST array over a ground plane," NTIA Report, TR-03-403, Jun. 2003.

[11] P. Bello, "Characterization of Randomly Time-Variant Linear Channels," *IEEE Trans. Communications Systems*, vol. 11, no. 4, pp. 360-393, Dec. 1963

[12] W. Jakes, Ed., *Microwave Mobile Communications*, Piscataway, NJ, IEEE Press, 1974.

[13] David Parsons, *The Mobile Radio Propagation Channel*, Halsted Press, New York, 1992, pp.111, pp. 129.

[14] William C.Y. Lee, "Estimate of local average power of a mobile radio signal," *IEEE Trans. Vehicular Tech.*, VT-34, NO. 1, Feb. 1985.

[15] R. Steel, *Mobile Radio Communications*, IEEE Press, New York, Pentech Press, London, 1992.

[16] Parsons, J.D., Ibrahim, M.F., "Signal strength prediction in built-up areas. Part 2: Signal variability," *Communications, Radar and Signal Processing, IEE Proceedings F*, vol. 130, no. 5, pp. 385-391, Aug. 1983.

[17] William C.Y. Lee, *Mobile Communications Engineering*, McGraw-Hill, New York, 1982.

[18] George Hufford, *Statisical Distributions*, Chapter 15, private communication.

[19] P.F. Wilson, P.B. Papazian, M.G. Cotton, and Y. Lo, "Advanced antenna test bed characterization for widenband wireless communications," NTIA Report 99-369, Aug. 1999.

[20] T.S. Rapport, "Characterization of UHF multipath radio channels in factory buildings," *IEEE Trans. Antennas and Propagation,* AP-37, pp. 1058-1069, Aug. 1989.

[21] S.Y. Seidel and T.S. Rappaport, "914 MHz path loss prediction models for indoor wireless communications in multifloored buildings," *IEEE Trans. Antennas and Propagation*, AP-40, pp.207-217, Feb. 1992.

[22] Yu-Shuan Yeh and Schwartz, S.,"Outage Probability in Mobile Telephony Due to Multiple Log-Normal Interferers," *IEEE Trans. Communications*, vol. 32, no. 4, pp. 380- 388, Apr. 1984.